Bioorganic Chemistry 133 (2023) 106408

Contents lists available at ScienceDirect

Bioorganic Chemistry

journal homepage: www.elsevier.com/locate/bioorg

Piperazine-derived small molecules as potential *Flaviviridae* NS3 protease inhibitors. *In vitro* antiviral activity evaluation against Zika and Dengue viruses

María del Rosario García-Lozano [a,b,1], Filippo Dragoni [c,1], Paloma Gallego [d,1], Sarah Mazzotta [e], Alejandro López-Gómez [a], Adele Boccuto [c,f], Carlos Martínez-Cortés [g], Alejandro Rodríguez-Martínez [h], Horacio Pérez-Sánchez [g], José Manuel Vega-Pérez [a], José Antonio Del Campo [i,*], Ilaria Vicenti [c,*], Margarita Vega-Holm [a,*], Fernando Iglesias-Guerra [a]

[a] Department of Organic and Medicinal Chemistry, Faculty of Pharmacy, University of Seville, E-41071 Seville, Spain
[b] SeLiver Group at the Institute of Biomedicine of Seville (IBIS), Virgen del Rocío University Hospital CSIC University of Seville, Seville, Spain
[c] Department of Medical Biotechnologies, Siena University Hospital, Policlinico Le Scotte, Viale Bracci 16, 53100 Siena, Italy
[d] Unit for Clinical Management of Digestive Diseases and CIBERehd, Valme University Hospital, 41014 Seville, Spain
[e] Department of Chemistry, University of Milan, 20133 Milan, Italy
[f] VisMederi Research srl, Siena, Italy
[g] Structural Bioinformatics and High Performance Computing (BIO-HPC) Research Group, UCAM Universidad Católica de Murcia, 30107 Murcia, Spain
[h] Department of Physical Chemistry and Institute of Biotechnology, University of Granada, Campus Fuentenueva sn, 18071 Granada, Spain
[i] ALGAENERGY S.A., Avda. Europa 19, 28108 Alcobendas, Madrid, Spain

ARTICLE INFO

Keywords:
Flavivirus
NS3 protease
Small molecules inhibitors
Privileged structures
Acyl and urea piperazine derivatives
Live virus phenotypic assay
Molecular docking
Molecular modeling

ABSTRACT

Since 2011 Direct Acting antivirals (DAAs) drugs targeting different non-structural (NS) viral proteins (NS3, NS5A or NS5B inhibitors) have been approved for clinical use in HCV therapies. However, currently there are not licensed therapeutics to treat *Flavivirus* infections and the only licensed DENV vaccine, Dengvaxia, is restricted to patients with preexisting DENV immunity.

Similarly to NS5 polymerase, the NS3 catalytic region is evolutionarily conserved among the *Flaviviridae* family sharing strong structural similarity with other proteases belonging to this family and therefore is an attractive target for the development of pan-flavivirus therapeutics.

In this work we present a library of 34 piperazine-derived small molecules as potential *Flaviviridae* NS3 protease inhibitors. The library was developed through a privileged structures-based design and then biologically screened using a live virus phenotypic assay to determine the half-maximal inhibitor concentration (IC_{50}) of each compound against ZIKV and DENV. Two lead compounds, **42** and **44**, with promising broad-spectrum activity against ZIKV (IC_{50} 6.6 μM and 1.9 μM respectively) and DENV (IC_{50} 6.7 μM and 1.4 μM respectively) and a good security profile were identified. Besides, molecular docking calculations were performed to provide insights about key interactions with residues in NS3 proteases' active sites.

Abbreviations: CC_{50}, half-maximal cytotoxic concentration; DCM, dichloromethane; DDAs, direct acting antivirals; DENV, Dengue virus; DEPT, distortionless enhancement by polarization transfer; DMF, dimethylformamide; DMSO, dimethylsulfoxide; EDCI, 1-ethyl-3-(3-dimethylaminopropyl)carbodiimide; ELISA, Enzyme-Linked Immunosorbent Assay; HCV, Hepatitis C virus; HIV, Human immunodeficiency virus; HOBt, hydroxybenzotriazole; HRMS, High resolution mass spectrometry; HSQC, heteronuclear single quantum correlation; IC_{50}, half maximal inhibitory concentration; MS, mass spectrometry; NMR, nuclear magnetic resonance; SARS–CoV–2, Severe acute respiratory syndrome coronavirus 2; SI, selectivity index; TLC, thin layer chromatography; TMS, tetramethylsilane; TPV, telaprevir; WHO, World Health Organization, ZIKV, Zika virus.

* Corresponding authors.
E-mail addresses: jcc@algaenergy.com (J. Antonio Del Campo), vicenti@unisi.it (I. Vicenti), mvegaholm@us.es (M. Vega-Holm).

[1] M.R.G-L, F.D, P.G joint as co-first authors.

https://doi.org/10.1016/j.bioorg.2023.106408
Received 27 July 2022; Received in revised form 23 January 2023; Accepted 1 February 2023
Available online 4 February 2023

1. Introduction

Flaviviridae family is subdivided into four genera namely, *Flavivirus, Hepacivirus, Pegivirus* and *Pestivirus*. *Flavivirus* genus includes prevalently arboviruses transmitted by infected arthropod, such as Dengue Virus (DENV), Japanese Encephalitis Virus (JEV), Yellow Fever Virus (YFV), Chikungunya Virus (CHIKV), Spondweni Virus (SPOV or SPONV), West Nile Virus (WNV) and Zika Virus (ZIKV) [1,2]. The incidence of Flavivirus infection has grown up to 400 million people infected annually [3] and widely distributed as consequence of globalization and climate changes, causing public health problems worldwide [4,5].

One of the most important pathogens of the *flaviviridae* family is the Hepatitis C virus (HCV) belonging to the *Hepacivirus* genus. Globally, an estimated 58 million people have chronic HCV infection, with about 1.5 million new infections per year and approximately 290,000 people died from hepatitis C in 2019, mostly from cirrhosis and hepatocellular carcinoma [6,7]. The absence of a vaccine and the possible emergence of viral resistance toward the drugs approved for HCV treatment, makes necessary the continuous design of novel specific HCV inhibitors which can implement the existing combination therapy.

DENV and ZIKV have an outstanding clinical and epidemiological relevance due to their high incidence and lack of effective treatments. DENV infections, has increased its global incidence dramatically (100–400 million infections each year) with about half of the world's population now at risk, particularly in developing countries [8,9]. Over 80% of infected patients are generally mild and asymptomatic [9] but approximately 5% have severe dengue with hemorrhagic fever [10]. Despite ZIKV infection usually proceeds asymptomatically or with mild symptoms, during the last outbreaks severe ZIKV-associated complications emerged (depending on genetic variant of ZIKV), such as congenital birth defects, including microcephaly, and the Guillain-Barre syndrome in adults [5]. In 2018, WHO has added ZIKV infection to its Research and Development Blueprint (the list of diseases recommended for intensive research) [8].

Currently no effective drugs [11] or vaccines against these diseases are available, the only vaccine approved against DENV, Dengvaxia is restricted to patients with preexisting DENV immunity and for this reason its distribution is limited to endemic area [11,12]. Therefore, at present the therapy for the treatment of DENV and ZIKV infections, includes only symptomatic treatment or supportive care in a hospital setting.

All genera of the *Flaviviridae* family show similarities in the organization of the viral genome, which is characterized by a single stranded positive sense RNA molecule. The whole viral genome is translated to a viral polyprotein which is processed by the host and viral proteases into 9 to 12 mature proteins, consisting of the structural and nonstructural (NS) proteins [1,12]. The structural proteins form the viral particle. The NS proteins participate in the replication of the RNA genome, virion assembly and interaction with innate host immune response [13]. These viral proteins represent relevant targets for the development of novel antiviral therapies. Novel *Flaviviridae* inhibitors has been designed to target NS3 (protease domain, helicase domain) and NS5 (*N*-terminal methyltransferase domain and C-terminal RNA-dependent RNA polymerase) viral proteins [14].

The NS3 protease domain belongs to the trypsin/chymotrypsin protease superfamily with a conserved catalytic triad consisted of His-Ser-Asp. During the viral lifecycle in host cell, the NS3 protease cleaves the polyprotein releasing the resulting NS proteins. The majority of NS protein structures are evolutionarily conserved among the *Flaviviridae* family [15], with strong structural similarity of the NS3 catalytic region [15–18], despite difference in NS3 cofactor usage; for example, NS4A acts as cofactor in HCV whereas NS2B is the cofactor in DENV and ZIKV [18]. In the research of new anti-*flavivirus* agents, the repurposing of HCV NS3/NS4A inhibitors for the treatment of ZIKV infections is a reported and appealing strategy [19].

In this work we present the design and the synthesis of a small library of 34 piperazine-derived small molecules acting as potential *Flaviviridae* NS3 protease inhibitors. The compounds were designed using a privileged structure-based approach and their antiviral properties were determined by a live virus cell based phenotypic assay against ZIKV and DENV allowing the identification of lead compounds with promising broad-spectrum activity against flaviviruses.

2. Results & discussion

2.1. Design

The design of the new antiviral compounds was based on our previous experience in the synthesis of piperazines as relevant scaffolds in anti-adenovirus activity [20,21]. In addition, the role of piperazine derivatives against *Flaviviridae* viruses such us HCV has also been reported [7,22–27]. Due to the relevance of the piperazine ring in the biological activity of compounds [28], we decided to preserve it as central core.

The general skeleton of the first family consisted of two aromatic/aliphatic rings assembled through amide [29] or urea [14,30] functions. The common structural feature is the 2-substituted piperazine ring as main backbone, with *tert*-butoxycarbonyl and its isostere 3,3-dimethylbutanoyl groups as acylating agents at N-4 [21,31]. The structural diversity generation was accomplished at N-1 by the introduction of moieties considered as relevant for the desired antiviral activity. Literature was consulted to identify some structural elements of interest that could be considered privileged structures for this activity (Fig. 1). We have recently employed this designing strategy for developing other antiviral agents based on different amine-propanediol skeletons with promising results [32,33].

Indol-3-yl-2-oxoacetyl, a biologically relevant oxoamide moiety [34–36] having the indole nucleus (privileged scaffold in ligands for diverse viral proteins) [36–38], that has been previously explored in anti-HIV agents [39], was selected for our model. Cinnamoyl and quinoline-3-carbonyl groups were also introduced at N-1 position in our general backbone. They are crucial pharmacophores that exhibit multiple biological activities [40–43], and important structural motifs in antiviral drug discovery against HCV [44,45], ZIKV [46–49], DENV [49–55] and SARS-CoV–2 [56].

In the second type of compounds, the urea spacer connects the privileged moiety with the N-1 of the piperazine ring.

To explore the chemical space around the urea scaffold, three different phenyl moieties were introduced. For the design of our library, 4-acetylphenyl [57,58], 2,4-dimethoxyphenyl [14] and 3,4,5-trimethoxyphenyl groups were selected based on their presence in small molecules aryl urea derivatives with potent anti ZIKV activity.

2.2. Synthesis

Compounds **8**–**31** were obtained following the previously described short and high-yielded synthetic methodology that involved two reactions [20,21,59], by employing 2-substituted piperazines as precursors. Firstly, through a chemoselective *N*-acylation reaction, the acyl function at the less hindered nitrogen was introduced (compounds **3**–**6**) Secondly, to generate chemical diversity at the other nitrogen, it was functionalized as amide and urea groups.

Thirdly, compounds **32**–**34** were prepared in one step from commercial Boc-piperazine by reaction with the appropriate acylating agents: acyl chloride or carboxylic acid.

The general synthetic route for these compounds is presented in Scheme 1. Spectral (NMR, Mass Spectrometry) and analytical data of the new synthesized compounds (**8**–**34**, Table 1) were in full agreement with the proposed structures (See Experimental Part and Supplementary Information).

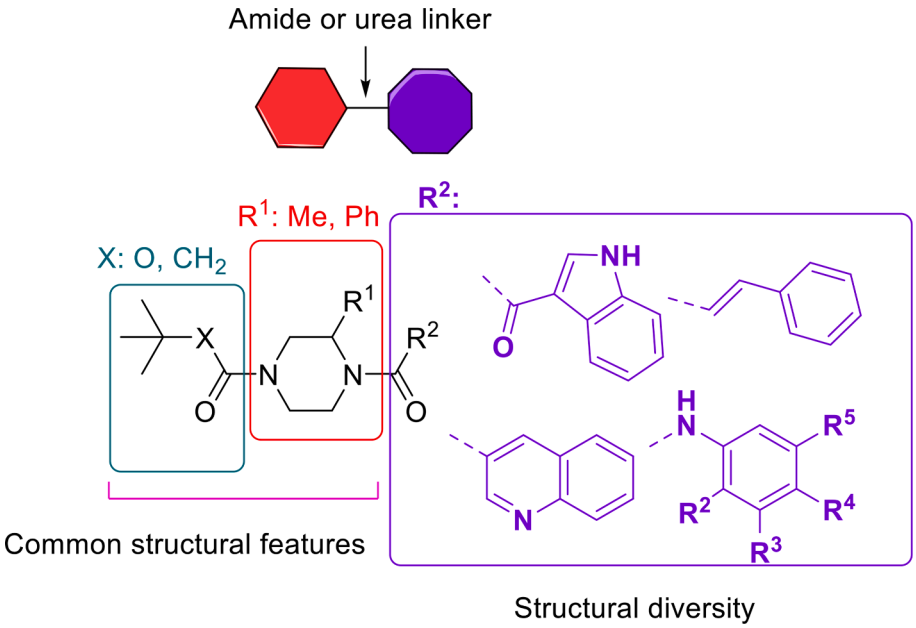

Fig. 1. Privileged structure-based design strategy for potential piperazine-derived anti-flavivirus agents.

2.3. Biological evaluation

2.3.1. In vitro protease inhibition assay

In the process of drug discovery, compounds exhibiting antiviral activity in cell based assays have better chance to be efficacious *in vivo* than in target-based approaches [60]. NS proteins in the *Flaviviridae* family, specifically the enzymes, are evolutionarily well conserved among different genera [8,61–64], existing a strong structural similarity in the catalytic region between the *Flavivirus* NS2B/NS3 and the HCV NS3/4A [15–18]. As our main goal was the development of broadly active antiviral compounds acting as pan *Flaviviridae* inhibitors, we started our antiviral drug discovery study by screening our library in a commercial HCV NS3/4A protease inhibition assay, to rapidly identify those compounds showing inhibitory enzymatic activity.

The rationale behind our approach is the fact that ZIKV inhibitors have been obtained by repurposing previously identified HCV NS3/NS4A inhibitors [19]. The discovery of novel broad spectrum compounds against HCV, *Flavivirus* and other viruses, by phenotypic screening starts with (i) anti-HCV cell-based viral infection screening, proceed with (ii) the optimizing process of anti HCV activity and it's completed with (iii) the evaluation of broad antiviral profile of leading compounds [65].

Compounds **8**–**34** were evaluated to determine their degree of inhibition of the NS3/4A protease activity of the HCV, using Telaprevir (TPV) as reference compound (for details see Experimental Part), obtaining data recorded in Table 1 (Supplementary Information, Graph S31).

As can be observed in Table 1, most of the HCV NS3/4A inhibitory values were >70%. Only five compounds gave around 40–50% of inhibition, being 2-phenyl piperazine derivatives having at N-1 a urea function with a 2,4-dimethoxy or 3,4,5-trimethoxy substituted phenyl ring (**25**, **30** and **31**) or an amide (3-quinolein carbonyl group in **29**, and cinnamoyl group in **21**).

2.3.2. Cytotoxicity and antiviral activity

It has been reported that some DENV inhibitors that exhibited inhibitory activities in biochemical protease assays, failed in cell-based viral infection assays [16,24]. This observation is not surprising considering that enzymatic assays evaluate only one activity of virus in a controlled reaction, while the viral replication in cell culture and consequently its inhibition, is a mechanism more complex which involves the interaction between different viral and cellular proteins.

Consequently, we screened the compounds with moderate-high percentage of enzymatic inhibitory activity in a cell-based antiviral assay, to determine their potential activity to inhibit ZIKV and DENV replication *in vitro*. The final goal was to find new lead compounds for hit optimization. Considering the enzymatic inhibition percentage data (Table 1) all compounds from the first family were evaluated.

The cell-based antiviral assay has been previously published [66,67] and it is explained in detail in the Experimental Section. Activity / toxicity data for compounds **8**–**34** are reported in the Table 2. The IC_{50} (half maximal inhibitory concentration) values obtained with the reference compound (sofosbuvir) were coherent with those obtained in literature and in previously published papers [66,68,69].

Anti-ZIKV activity was observed in the micromolar range, in 11 out 27 compounds that compose the library with a median [IQR] IC_{50} of 24 [8.4–37.0] μM and a mean SI of 10 [6.4–14.0]. Six of them were 2-methyl piperazine derivatives (**8**, **11**, **14**, **15**, **16** and **18**). Both *tert*-butoxycarbonyl and 3,3-dimethylbutanoyl groups are present in active compounds at N-4. Related to the different moieties at N-1, amide-linked derivatives with indol-3-yl-2-oxoacetyl (**8** and **14**), cinnamoyl (**15**) and quinoline-3-carbonyl (**16**), together with urea-linked compound with 4-acetylphenyl (**11**) showed a good SI, with a median SI of 10.2 [13.3–17.1] (Table 2) [70].

Only three 2-phenylpiperazine were active: both 3,4,5-trimethoxyphenyl urea derivatives (IC_{50} **24** 8.2 μM and **29** 41.2 μM, with *tert*-butoxycarbonyl and 3,3-dimethylbutanoyl groups respectively at N-4) and **25**, indol-3-yl-2-oxoacetyl derivative with IC_{50} 3.9 μM. Of them, only the compound **24** had a low cytotoxic profile (SI = 14.6).

Three different unsubstituted Boc-piperazine derivatives, **32**, **33** and **34**, featuring the indol-3-yl-2-oxoacetyl, cinammoyl and indol-3-yl-acetyl respectively at the other N, were also prepared. Compound **32**, unsubstituted analogue of **8** was not active, while compound **34**, with the indol-3-yl acetyl group showed a poor activity (IC_{50} 51.9 μM). Compound **33** showed certain activity (IC_{50} 24.2 μM) while its 2-substituted analogues **9** and **21** were inactive.

These results suggested that the presence of 2-metylpiperazine core in our model is crucial for the activity against ZIKV.

At opposite of compounds active againt ZIKV, most of the compounds containing 2-methylpiperazine moiety were inactive against

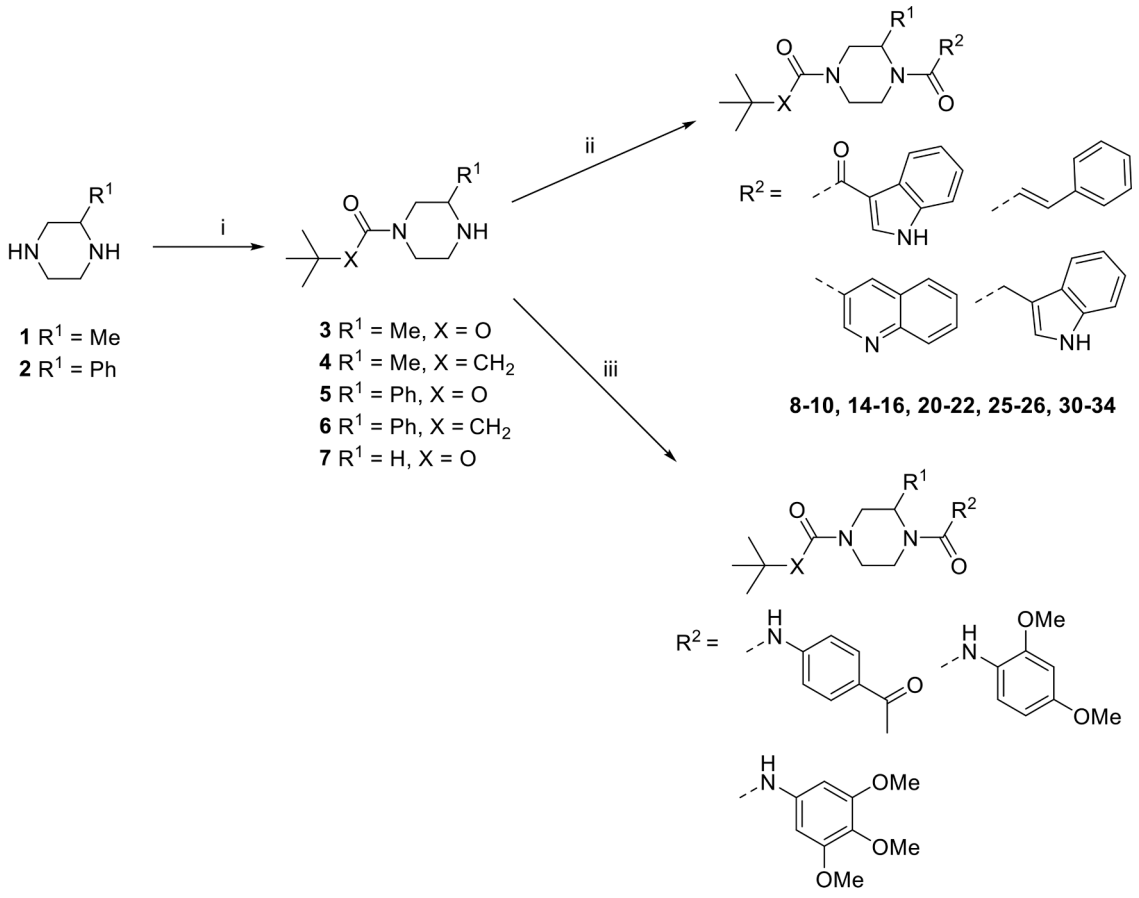

i: starting material 1 eq, acyl halyde or anhydride 1 eq, piridine 2 eq, CH_2Cl_2
ii: monoamide 1 eq, carboxylic acid 1.3 eq, EDCI 1.5 eq, HOBt 1.7 eq, DMF; or monoamide 1 eq, acyl halyde 1.2 eq, piridine 1.5 eq, CH_2Cl_2
iii: monoamide 1 eq, isocyanate 1.2 eq, CH_2Cl_2

Scheme 1. Synthesis of 2-substituted piperazine amide and urea derivatives (**8**–**31**) and unsubstituted piperazine derivatives (**32**–**34**).

DENV, with the exception of the indol-3-yl-2-oxoacetyl derivatives, compound **8** (IC_{50} 10.7 μM, SI 14.3) and **14** (IC_{50} 26.0 μM, SI 7.7) which showed a similar activity profile against ZIKV.

The activity profile changed when 2-phenylpiperazine core was present. Six out eleven prepared derivatives displayed anti DENV activity. Indeed, compounds **21**, **22**, **23**, **25**, **26** and **29** showed IC_{50} values ranging from 7.9 to 31.3 μM. However, considering their median SI 4.2 [3.1–4.7], probably they require further optimization to reduce their cytotoxicity.

Among the three (**32**–**34**) unsubstituted piperazine derivatives evaluated, only two presented low activity, compund **32** with indol-3-yl-2-oxoacetyl group (IC_{50} 45.0 μM) and its analogue **34** with indol-3-yl-acetyl (IC_{50} 38.7 μM) which was similarly active against ZIKV.

Globally, **8** was the most promising tested compound, considering its activity in the low micromolar range against both viruses and its low cytotoxic profile. As our compounds were prepared in racemic form, both enantiomers of compound **8** were evaluated in the cell-based assay to determine their inhibitory activity against ZIKV and DENV replication [**(*R*)-8** $[\alpha]_D = -8.0$ (c 1.04, CH_2Cl_2), **(*S*)-8** $[\alpha]_D = +8.1$ (c 0.95, CH_2Cl_2)]. Not substantial differences (Fig. 2) were appreciated among their IC_{50} values against ZIKV [**(*R*)-8** 13.8 ± 1.2 μM, **(*S*)-8** 12.7 ± 1.4 μM)] and DENV [**(*R*)-8** 12.7 ± 1.2 μM, **(*S*)-8** 11.2 ± 1.3 μM)], showing almost similar activities and cytotoxicity (SI > 10) to those obtained with the racemic form.

As both enantiomers of compound **8** showed similar activity profile in cell-based assay against ZIKV and DENV replication, a docking study was performed to look inside the binding mode of both enantiomers with the active site of Zika NS3/2B and to check the differences between (*R*) and (*S*) configurations. The groups in the chiral carbon do not present interactions with any residues, and the interactions in the two enantiomers are similar in both cases with similar binding energy values (Supplementary Information, Fig. S32).

2.4. Round of optimization

A further round of optimization was performed to obtain a second small family of inhibitors. The goal was to increase the molecular complexity through the assembly of 3 aromatic/aliphatic rings linked by both functions, urea and amide, in the same molecule.

In pursuit of improving the antiviral activity against both viruses and reducing the cytotoxicity of those lead compounds, the first decision was to preserve 2-phenylpiperazine ring as the central core, due to its relevance for anti-DENV activity.

The following chemical construction process focused on the incorporation of two biologically interesting motifs to both nitrogen atoms of the piperazine ring located at central position The scaffold's selection

Table 1
Acyl piperazine amide and urea derivatives (**8**–**34**). Inhibition of HCV NS3/4A protease.

Entry	Comp	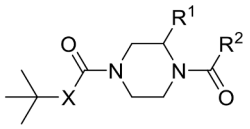				
		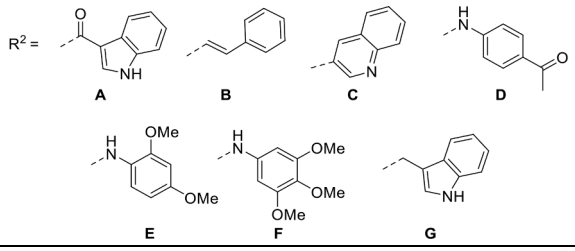				
		R^1	X	R^2	Yield (%)	% Enzimatic Inhibition[a]
1	**8**	Me	O	A	64	73.98 ± 8.59
2	**9**	Me	O	B	67	77.87 ± 11.42
3	**10**	Me	O	C	94	76.12 ± 2.23
4	**11**	Me	O	D	79	77.13 ± 13.64
5	**12**	Me	O	E	68	86.20 ± 9.30
6	**13**	Me	O	F	61	78.71 ± 15.45
7	**14**	Me	CH_2	A	61	76.71 ± 14.91
8	**15**	Me	CH_2	B	62	83.18 ± 6.06
9	**16**	Me	CH_2	C	88	68.29 ± 0.29
10	**17**	Me	CH_2	D	76	79.15 ± 9.66
11	**18**	Me	CH_2	E	77	83.76 ± 11.74
12	**19**	Me	CH_2	F	68	76.14 ± 3.31
13	**20**	Ph	O	A	63	75.92 ± 4.05
14	**21**	Ph	O	B	71	51.05 ± 10.05
15	**22**	Ph	O	C	90	ND[b]
16	**23**	Ph	O	E	83	79.19 ± 7.93
17	**24**	Ph	O	F	69	41.90 ± 20.19
18	**25**	Ph	CH_2	A	72	81.05 ± 1.75
20	**26**	Ph	CH_2	C	79	ND[b]
21	**27**	Ph	CH_2	D	91	44.92 ± 15.71
22	**28**	Ph	CH_2	E	72	47.66 ± 23.99
23	**29**	Ph	CH_2	F	65	47.39 ± 18.03
24	**30**	Me	O	G	74	ND[b]
25	**31**	Ph	O	G	81	61.92 ± 4.45
26	**32**	H	O	A	94	80.87 ± 0.76
27	**33**	H	O	B	79	86.90 ± 0.79
28	**34**	H	O	G	78	85.32 ± 0.12
29	**TVP**	–	–	–	–	88.41 ± 5.82

[a] Percent inhibitory activity of compounds on HCV NS3/4A protease (genotype 1b) at 0.5 mM. All results are shown as means ± SD of triplicate samples from three independent experiments. See Experimental Section for details.
[b] Not determined.

preserved the structural features of the most active compounds from the previous family (Fig. 3):

(1) For the amide link, indol-3-yl-2-oxoacetyl and cinammoyl groups carried in compunds **8**, **21** and **25**.
(2) For the urea connection, the 2,4-dimethoxyphenyl ring presents in compounds **18** and **23**, and the 4-acetylphenyl, evaluated in 2-methyl piperazine derivatives (**11**), but not previously incorporated to 2-phenylpiperazine core. The third moiety was (2-chloro-5-trifluoromethyl) phenyl, based on the fact that urea derivatives having this group have been described as effective anti ZIKV compounds [58].

It is also important to consider the relative position of the substituent at position 2 in the piperazine ring and the privileged scaffolds linked to the nitrogen atoms.

Firstly, two indol-3-yl-2-oxoacetyl derivatives were prepared starting from compounds **8** and **20** (2-methyl and phenyl derivatives respectively), which yielded compounds **37** and **38** through the deprotection of the Boc group by treatment with CF_3COOH (**35** and **36**), followed by reaction with the appropriate isocyanate (Scheme 2).

The groups indol-3-yl-2-oxoacetyl and cinammoyl were introduced at the less hindered nitrogen through a chemoselective *N*-acylation reaction (**39** and **40)** and secondly, N-1 was functionalized as urea to introduce the biologically relevant scaffolds mentioned above (**41**–**44**). All these compounds were obtained in high yields and their spectral and analytical data confirmed the proposed structure (See Experimental Section) (Scheme 2).

The lead compounds, improved with the above-mentioned modifications, were tested in cells-based assay to assess their cytotoxic profile and their antiviral activity (Table 3, Fig. 4).

As illustrated in Table 3, compound **37**, the only 2-methyl derivative of this family, showed a modest activity against both viruses (mean IC_{50} 33.5 μM when considering both ZIKV and DENV). Among the 3-phenyl-derivatives (**38, 41** and **43**) carrying the indol-3-yl-2-oxoacetyl group the cytotoxicity ranging from moderate to high. Indeed the compound

Table 2
Cytotoxic profile and antiviral activity of acyl piperazine amide and urea derivatives (**8**–**34**) *in vitro*. Sofosbuvir, tested in each assay was used as reference control. Experiments were performed in Huh7 cell line.

Comp	CC_{50}[a] (μM)	IC_{50}[b] (μM) ZIKV	SI[c] ZIKV	IC_{50}[b] (μM) DENV	SI[c] DENV
8	153	8.9 ± 1.2	17.1	10.7 ± 2.0	14.3
9	123	NA[d]	–	NA	–
10	110	NA	–	NA	–
11	200	11.6 ± 1.3	17.3	NA	–
12	200	NA	–	NA	–
13	200	NA	–	NA	–
14	200	20.6 ± 1.2	9.7	26.0 ± 3.4	7.7
15	200	15.0 ± 1.2	13.3	NA	–
16	84	8.0 ± 1.3	10.2	NA	–
17	>200	NA	–	NA	–
18	200	58.2 ± 1.5	3.4	NA	–
19	200	NA	–	NA	–
20	15.3	NA	–	NA	–
21	21.5	NA	–	7.9 ± 3.0	2.7
22	60	NA	–	14.8 ± 0.2	4.1
23	95	NA	–	14.6 ± 3.3	6.5
24	115	8.2 ± 1.2	14.6	NA	–
25	20	3.9 ± 0.2	5.1	9.0 ± 6.6	2.2
26	112	NA	–	22.7 ± 7.5	4.9
27	47.3	NA	–	NA	–
28	60	NA	–	NA	–
29	130	41.2 ± 11.3	3.2	31.3 ± 3.5	4.2
30	100	NA	–	NA	–
31	18.7	NA	–	NA	–
32	130	NA	–	45.0 ± 1.4	2.9
33	200	24.2 ± 1.9	8.3	NA	–
34	200	51.9 ± 19.4	7.7	38.7 ± 2.0	10.3
Sofosbuvir	>200	4.0 ± 1.3	100.0	13.1 ± 1.2	30.5

[a] Half-maximal cytotoxic concentration (CC_{50}). The results represent means of triplicate experiments.
[b] Half maximal inhibitory concentration (IC_{50}). The results represent means ± standard deviation of 2 independent experiments performed in triplicate.
[c] The selectivity index value was determined as the ratio of CC_{50} to IC_{50} for each compound.
[d] NA. Not active.

43, was completely toxic in cell culture while the **41** had a low SI (1.6) despite its anti DENV activity was in the low micromolar range (IC_{50} 7.3 μM). Compound **38**, carrying the indol-3-yl-2-oxoacetyl group at N-1 and the 2,4-dimethoxyphenyl urea at N-4 had a good anti-DENV activity (IC_{50} 2.2 μM), with a SI of 14.5 which can be improved in future reducing its cytotoxicity (32 μM). The most promising compounds were the **42** and the **44,** carrying the cinammoyl group at N-4. Indeed, they inhibited robustly the ZIKV and DENV replication with IC_{50} in the low micromolar range and high SI (60.5/59.7 ZIKV/DENV for compound **42** and 33.5/44.6 ZIKV/DENV for compound **44**).

Thus, the optimization process led to the development of two promising pan-flavivirus agents with anti-DENV activity higher than that recorded by reference compound sofosbuvir in cell culture.

2.5. Docking studies

To further establish whether the inhibitors targeted the viral protease as we hypothesized, molecular docking analyses on **8**, **42** and **44,** the most promising compounds of both libraries, were performed.

2.5.1. HCV NS3 protease molecular modeling

The docking scores and the interactions snapshot for the three compounds were obtained using PLIP [71] and PyMOL [72] software. These were found in the HCV NS3/4A Protease active site [73] with scores of −6.75 kcal/mol, −6.53 kcal/mol and −6.01 kcal/mol, for compounds **8**, **42** and **44**, respectively. In addition, the compounds were found close to the active site [74] (Fig. 5), and some interactions with the essential catalytic residues (His76, Asp100 and Ser158) [72] were detected (Supplementary Information, Table S33).

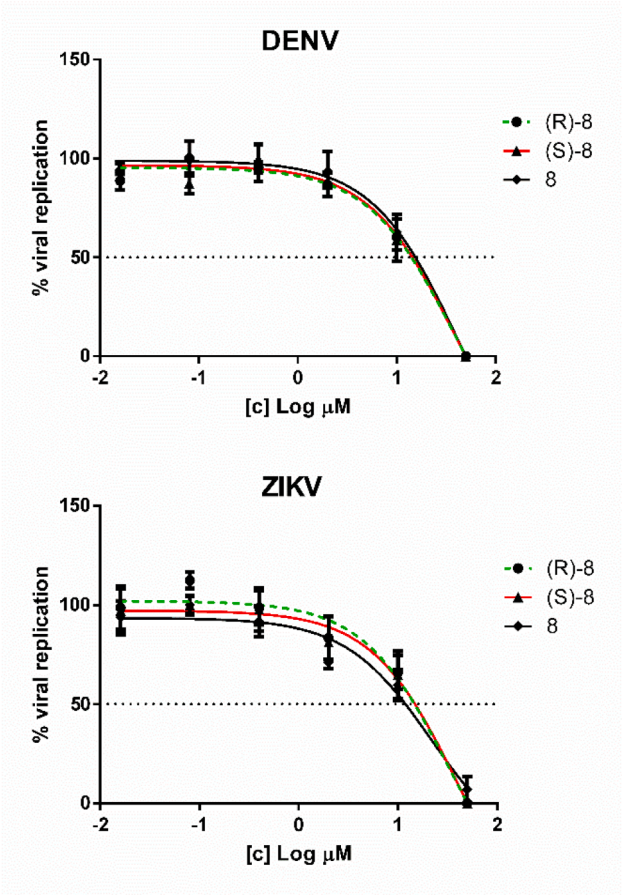

Fig. 2. Inhibitory activity of compound **8** and its enantiomers, (***R*)-8** and (***S*)-8** against ZIKV and DENV in cell culture. The micromolar compound concentration is expressed as logarithm on x-axis, the viral replication is expressed on y-axis as percentage. The normalized curve for each compound derives from 2 independent experiments performed in triplicate.

And additional docking study was performed to evaluate the potential interaction of the ketoamide group present in **8** (indol-3-yl-2-oxoacetyl derivative) with residues of the active site in the protease. This compound was compared to **30** (indol-3-yl-acetyl derivative, analogue to **8**). Compound **8** shows two interactions in Ser 158, with both carbonyl groups, amide and ketone. Compound **30** only interacts with this residue once through the carbonyl in the amide function (Supplementary Information Fig. S34).

2.5.2. ZIKV NS3 protease molecular modeling

In the case of ZIKV NS3/2B protease, the docking scores for the three compounds were similar to HCV protease scores with values of −5.61, −5.78 and −5.79 kcal/mol for compounds **8**, **42** and **44**, respectively (Supplementary Information, Table S35).

In addition, the interactions obtained were related to critical residues for this active site, which consisted of the following residues: His77, Ser161, Tyr176, Tyr187 [75] (Fig. 6).

These results support their expected mechanism of action as protease inhibitors.

2.6. In silico prediction of physicochemical and pharmacokinetic properties

In the drug development process, most of the new drug candidates fail in clinical trials due to their reduced ADME properties. In early stages of this process is critical to assess pharmacokinetic properties

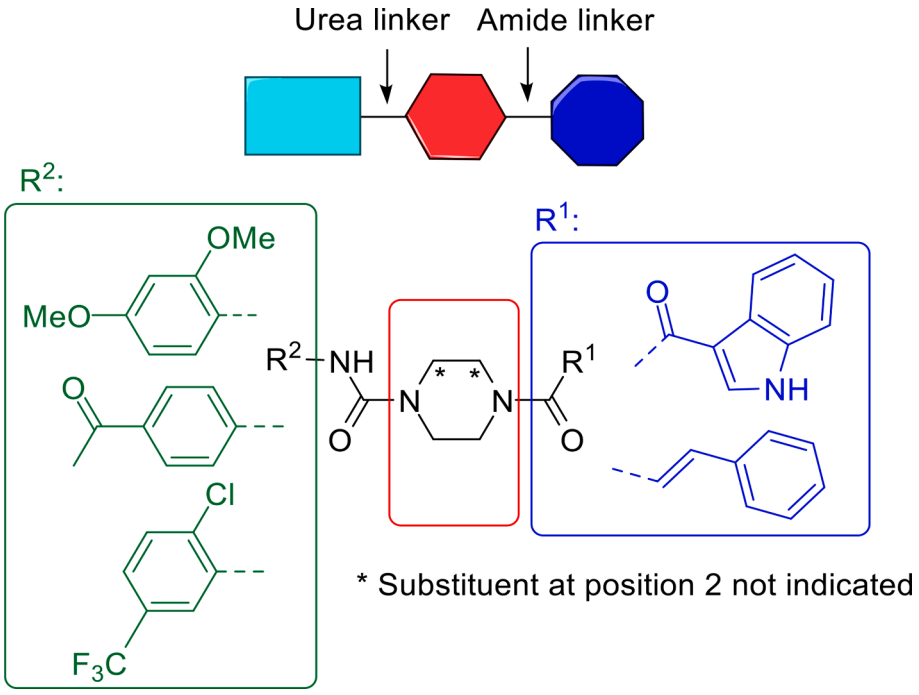

Fig. 3. Privileged structure-based optimization process.

prediction, to minimize the risk of drug attrition in late stage, related to poor ADME profiles. In this sense, *in silico* ADME screens provide a good starting point to select the most promising candidates for development and to reject those with low chance of success [76].

Based on previously discussed results, the 2 lead compounds (**42 and 44**) and different compounds showing activity against both viruses (**8**, **14**, **34** and **37**), or active against only one virus but with a good SI (**11, 15, 16, 24 and 38**) were submitted to *in silico* ADME properties evaluation.

Compounds were first tested for drug-likeness by Lipinski's Rule of Five [77–79]. SwissADME was the software used to predict the afore mentioned physicochemical parameters of the selected compounds (Table S36, Supplementary Information) [80].

Excepting compound **44** (with molecular weight > 500 and log P > 5), the investigated compounds were satisfying to Lipinski's rule of five [81,82].

Molsoft was used to predict drug likeness model scores of the compounds (Table S36, Supplementary Information). (Available from: URL: https://www.molsoft.com/) [81]. The more positive drug likeness score values, the more likely the compound was expected to be as a promising therapeutic pharmacophore [83]. A positive model score was attributed for the most promising compounds **38**, **42** and **44** (score ranged from 0.59 to 1.09).

Prediction of the major pharmacokinetic parameters such as absorption and distribution, were estimated using Pre-ADMET software (Available from: URL: http://preadmet.bmdrc.org) [84,85]. The outcomes of the predicted ADME parameters (Table S37, Supplementary Information) indicate good pharmacokinetic profile and drug likeness.

3. Conclusions

In summary, a library of 34 piperazine-derived small molecules have been described. They have been designed employing a privileged-structures based strategy through the incorporation of a 2-substituted piperazine ring (main backbone) which is considered relevant for exerting antiviral activity as protease inhibitors of viruses belonging to the *Flaviviridiae* family.

The compounds were firstly screened by a commercial HCV NS3/4A protease inhibition assay, recording inhibitory values above 70%, and then, to determine their potential activity to inhibit ZIKV and DENV replication *in vitro*, they were evaluated in a cell-based antiviral assay. From this library, compound **8** (general structure based on two rings assembled) was the most promising, being active in the low micromolar range against both viruses and poorly cytotoxic. A further round of optimization increasing the molecular complexity, led to the development of two compounds, the **42** and the **44** with a general structure based on three rings assembled. Both compounds had an anti-DENV activity higher than those recorded by reference compound sofosbuvir in cell culture, and a good security profile. The molecular docking analyses on compounds **8**, **42** and **44** showed compound residues interacting with both HCV NS3/4A and ZIKV NS3/2B protease active sites, supporting their expected mechanism of action as protease inhibitors. These compounds based on the piperazine scaffold structure can be considered as promising hit candidates for the development of a new class of pan *Flavivirus* agents. Further chemical exploration of this scaffold will be performed to search potent antiviral agents with broad spectrum activity against flaviviruses.

4. Experimental Section

4.1. Chemistry

4.1.1. General chemistry methods

All reagents, solvents, and starting materials were obtained from commercial suppliers and used without further purification. The crude reaction mixtures were concentrated under reduced pressure by removing the organic solvents in a rotary evaporator (BÜCHI R-200). Reactions were monitored by thin layer chromatography (TLC) using Kieselgel 60 F_{254} (E. Merck) plates and UV detector (SPECTROLINE MODEL CM-10) for visualization. Flash column chromatography was performed on Silica Gel 60 (E. Merck, 0,040–0,063 mm) and sea sand washed (Panreac, thin grade ~ 0,25–0,30 mm), with the indicated eluent. All reported yields are of purified products. Melting points were obtained on a GALLENKAMP Melting Point Apparatus MPD350.BM2.5 with open capillaries (Kimax-51°, 1.5–1.8 × 90 mm) and are uncorrected. Mass spectra were recorded on a Orbitrap Elite (Thermo

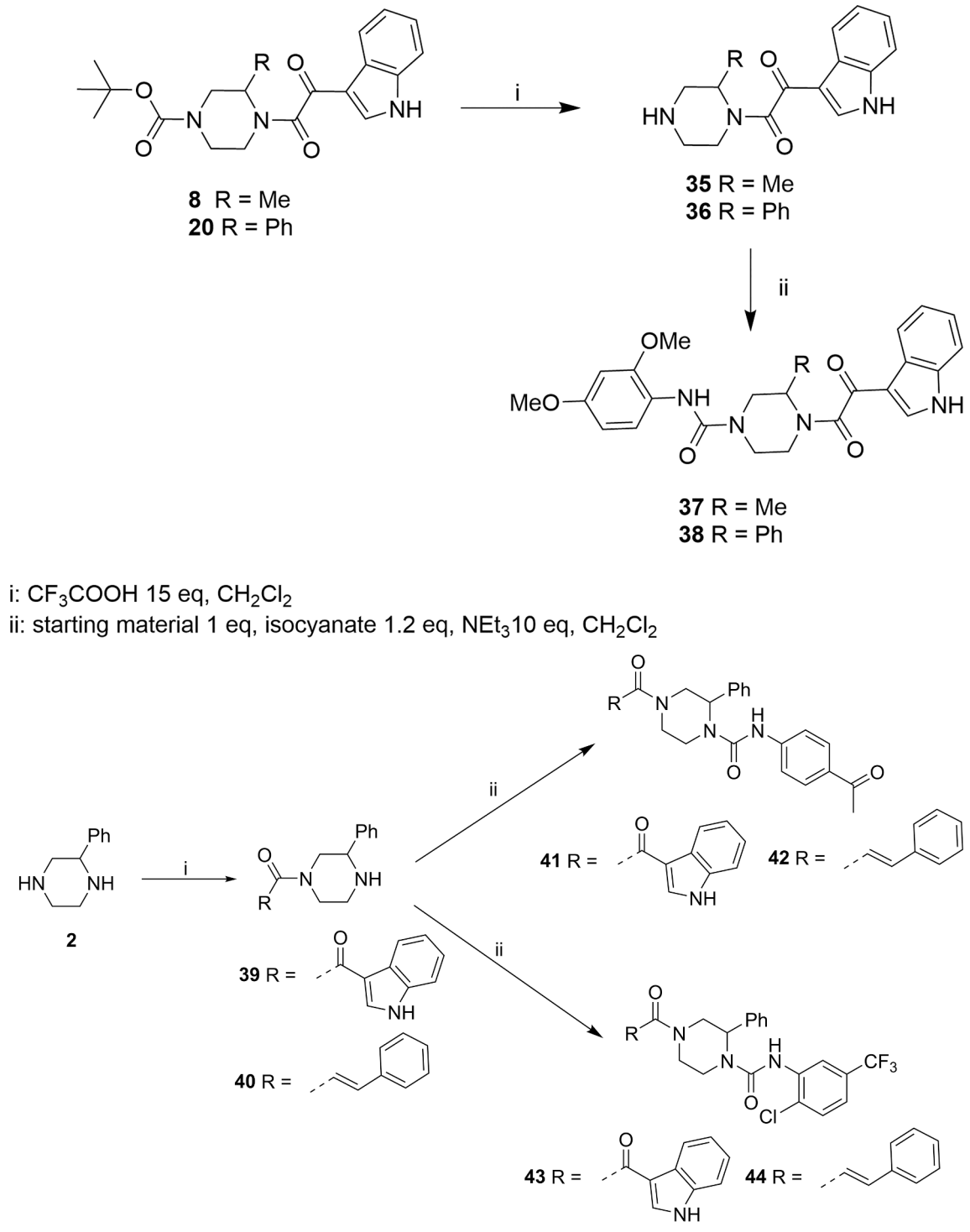

Scheme 2. Synthesis of optimized compounds **37**, **38**, **41**–**44**.

Scientific), a Hybrid Ion trap-orbitrap mass spectrometer capable of acquiring with a resolution higher than 240000, with ESI, HESI, APCI and nanoESI ionization sources. NMR spectra were recorded at 25 °C on a Bruker AV500 spectrometer at 500 MHz for ^{1}H and 125 MHz for ^{13}C. The chemical shifts (δ) reported are given in parts per million (ppm) and the coupling constants (J) are in hertz (Hz). ^{1}H chemical shift values (δ) are referenced to the residual non deuterated components of the NMR solvents (δ = 2.54 ppm for DMSO-d_6). The ^{13}C chemical shifts (δ) are referenced to DMSO-d_6 (central peak, δ = 39.5 ppm) as the internal standard. The spin multiplicities are reported as s (singlet), d (doublet), t (triplet), q (quadruplet), m (multiplet), or bs (broad singlet). COSY, DEPT, HSQC experiments were performed to assign the signals in the NMR spectra. The purity of final compounds was evaluated by C, H, N, S elementary analysis on a LECO TruSpec Micro CHNS (Maximum combustion temperature: 1050 °C). The purity of the final compounds was confirmed to be ≥95% by combustion.

Table 3
Cytotoxic profile and antiviral activity of optimized compounds **37**, **38**, **41**–**44** *in vitro*. Sofosbuvir, tested in each assay was used as reference control. Experiments were performed in Huh7 cell line.

Comp	CC_{50}[a] (μM)	IC_{50}[b] (μM) ZIKV	SI[c] ZIKV	IC_{50} (μM) DENV	SI[c] DENV
37	>200	31.7 ± 5.4	12.6	35.2 ± 15.1	11.4
38	32	NA[d]	–	2.2 ± 1.1	14.5
41	12	NA[d]	–	7.3 ± 2.8	1.6
42	>200	6.6 ± 1.4	60.5	6.7 ± 2.6	59.7
43	Toxic	–	–	–	
44	62	1.9 ± 0.4	33.5	1.4 ± 0.3	44.6
Sofosbuvir	>200	4.7 ± 1.2	85.1	12.1 ± 1.3	33.1

[a] Half-maximal cytotoxic concentration (CC_{50}). The results represent means of triplicate experiments.
[b] Half-maximal inhibitory concentration (IC_{50}). The results represent means ± Standard deviation of 2 independent experiments performed in triplicate.
[c] The selectivity index value was determined as the ratio of CC_{50} to IC_{50} for each compound.
[d] NA: Not active.

4.1.2. General procedure 1. Chemoselective N-acylation reaction of 2-substituted piperazines (3–6, 39, 40)

2-Substituted piperazine (5.0 mmol) was dissolved in dry dichloromethane (100 mL) and cooled to 0 °C. A solution of the appropriate acylating agent (5.0 mmol) in dichloromethane (20 mL) was added dropwise in 30 min, and then pyridine (10 mmol). The reaction mixture was kept into an ice-water bath with stirring 6 h and left at room temperature until TLC showed that all the starting material had reacted. The reaction mixture was evaporated to dryness to obtain the corresponding monoacyl derivative. Flash column chromatography gave the pure compound in high yield.

4.1.2.1. 1-(tert-Butoxycarbonyl)-3-methylpiperazine (3) [20,21]. The product was obtained as an oil and purified by column chromatography using ethyl acetate–methanol (10:1) as eluent (930 mg, 93% yield).^{1}H NMR (500 MHz, DMSO-d_6) δ 3.75–3.7 1 (m, 2H), 2.85–2.82 (m, 1H), 2.75–2.69 (m, 1H), 2.60–2.54 (m, 3H), 2.39–2.34 (m, 1H), 1.41 (s, 9H), 0.96 (d, J = 6.3 Hz, 3H). ^{13}C NMR (125 MHz, DMSO-d_6) δ 154.5, 79.3, 51.2, 50.5, 45.5, 44.4, 28.6, 19.3. HRMS (*m/z*): calcd for $C_{10}H_{20}N_2O_2$ 200.1528 $[M]^+$; found 200.1525.

4.1.2.2. 1-(3,3-Dimethylbutanoyl)-3-methylpiperazine (4) [21]. The product was obtained as an oil and purified by column chromatography using ethyl acetate–methanol (5:1) as eluent (861 mg, 87% yield). ^{1}H NMR (500 MHz, $CDCl_3$) δ 4.57 (d, J = 12.4 Hz, 1H), 3.85 (m, 1H), 3.52–3.08 (m, 2H), 3.06–2.62 (m, 3H), 2.23 (s, 2H), 1.33 (bs, 3H), 1.02 (s, 9H). ^{13}C NMR (125 MHz, $CDCl_3$) δ 170.3, 51.4, 45.8, 44.6, 44.5, 39.3, 31.5, 30.0, 17.3. HRMS (*m/z*): calcd for $C_{11}H_{22}N_2ONa$ 221.1624 $[M + Na]^+$; found 221.1619.

4.1.2.3. 1-(tert-Butoxycarbonyl)-3-phenylpiperazine (5) [20,21]. The product was obtained as a solid and purified by column chromatography using ethyl acetate–methanol (100:1) as eluent (1.26 g, 96% yield), mp 130–133 °C. ^{1}H NMR (500 MHz, $CDCl_3$) δ 7.4–7.3 (m, 5H), 4.05 (bs, 2H), 3.70 (dd, J = 2.4 Hz, J = 10.5 Hz, 1H,), 3.07 (m, 1H), 2.9–2.8 (m, 2H), 2.72 (bs, 1H), 1.90 (bs, 1H), 1.47 (s, 9H). ^{13}C NMR (125 MHz, $CDCl_3$) δ 154.8, 141.5, 128.5, 127.8, 127.0, 79.7, 60.3, 51.5, 46.1, 43.4, 28.5. HRMS (*m/z*): calcd for $C_{15}H_{23}N_2O_2$ 263.1754 $[M + H]^+$; found 263.1748.

4.1.2.4. 1-(3,3-Dimethylbutanoyl)-3-phenylpiperazine (6) [21]. The product was obtained as an oil and purified by column chromatography using ethyl acetate–methanol (20:1) as eluent (1.27 g, 97% yield). ^{1}H NMR (500 MHz, DMSO-d_6) δ 7.45–7.27 (m, 5H), 4.44–4.39 (m, 1H), 3.94–3.85 (m, 1H), 3.58 (dd, J = 2.3 Hz, J = 10.3 Hz, 1H), 3.31 (bs, 1H), 3.11–2.99 (m, 2H), 2.91–2.68 (m, 1H), 2.61–2.57 (m, 1H), 2.31–2.20 (m, 2H), 1.02, 1.00 (2 s, 9H). ^{13}C NMR (125 MHz, DMSO-d_6) δ 169.3, 169.2, 142.2, 141.9, 128.2, 128.1, 127.4, 127.3, 127.0, 126.9, 60.1, 59.4, 53.5, 48.1, 46.4, 45.9, 45.5, 43.8, 43.6, 41.1, 40. HRMS (*m/z*): calcd for $C_{16}H_{25}N_2O$ 261.1889 $[M + H]^+$; found 261.1886.

4.1.2.5. 1-[2-(Indol-3-yl)-2-oxoacetyl]-3-phenylpiperazine (39). The product was obtained as an oil and purified by column chromatography using dicholormethane-methanol (60:1) as eluent (1.1 g, 64% yield). ^{1}H NMR (500 MHz, DMSO-d_6) δ 12.36 (s, 1H), 8.21 (bs, 1H), 8.17–8.09 (m, 1H), 7.59–7.20 (m, 7H), 4.42–4.34 (m, 1H), 3.85–3.61 (m, 1H), 3.55–3.42 (m, 1H), 3.24–2.66 (m, 5H). ^{13}C NMR (125 MHz, DMSO-d_6) δ 186.3, 186.2, 165.8, 141.7, 141.1, 137.1, 137.0, 136.9, 128.4, 128.3, 127.5, 127.4, 126.9, 126.7, 124.0, 124.7, 123.6, 122.5, 120.9, 120.8, 113.6, 113.1, 112.6, 60.9, 59.1, 52.9, 47.6, 46.1, 45.8, 45.1, 41.0. HRMS (*m/z*): calcd for $C_{20}H_{20}N_3O_2$ 333.1477 $[M + H]^+$; found 333.1473.

4.1.2.6. 1-Cinnamoyl-3-phenylpiperazine (40). The product was obtained as an oil and purified by column chromatography using hexane–ethyl acetate (1:7) as eluent (1.4 g, 97% yield). ^{1}H NMR (500 MHz, DMSO-d_6) δ 7.75–7.30 (m, 12H), 4.52–4.43 (m, 1H), 4.35–4.23 (m, 1H), 3.76–3.63 (m, 2H), 3.56–3.25 (m, 2H), 3.12–0.66 (m, 2H); ^{13}C NMR (125 MHz, DMSO-d_6) δ 164.5, 141.6, 135.2, 129.5, 128.7, 128.3, 128.2, 128.1, 127.5, 127.3, 126.9, 118.3, 60.2, 59.4, 52.1, 48.9, 46.2, 45.5, 45.3, 41.8. HRMS (*m/z*): calcd for $C_{19}H_{20}N_2ONa$ 315.1473 $[M + Na]^+$; found 315.1456.

4.1.3. General procedure 2. Synthesis of N,N'-diacyl derivatives

(A) By reaction with acyl halide. To a solution of the monoacyl derivatives (**3**–**7**) (1.0 mol) in dry dichloromethane (15 mL) was added the corresponding acyl halide (1.2 mmol) and dry pyridine (1.5 mmol). The reaction mixture was stirred at room temperature under argon atmosphere until TLC showed that all the starting material had reacted. The reaction mixture was diluted in dichloromethane and successively washed with hydrochloric acid solution 1 M, saturated solution of sodium bicarbonate, dried (Na_2SO_4), filtered and the filtrate was evaporated to dryness. The compounds obtained were purified by flash chromatography.

4.1.3.1. 4-(tert-Butoxycarbonyl)-1-[2-(indol-3-yl)-2-oxoacetyl]-2-methylpiperazine (8). The product was obtained as a solid and purified by column chromatography using hexane–ethyl acetate (1:1) as eluent (237 mg, 64% yield), mp 223–225 °C. ^{1}H NMR (500 MHz, DMSO-d_6) δ 12.31, 12.29 (2bs, 1H), 8.22–8.10 (m, 2H), 7.55 (d, J = 7.4 Hz, 1H), 7.33–7.25 (m, 2H), 4.67 (m, 1H), 4.31–3.69 (m, 4H), 3.06–2.70 (m, 2H), 1.42 (s, 9H), 1.22, 1.15 (2d, J = 6.7 Hz, 3H). ^{13}C NMR (125 MHz, DMSO-d_6) δ 186.1, 186.0, 166.0, 165.9, 154.2, 137.2, 137.0, 136.9, 124.8, 123.6, 122.5, 120.9, 120.8, 113.0, 112.9, 112.6, 79.2, 49.3, 43.9, 40.7, 35.3, 27.9, 15.6, 14.8. HRMS (*m/z*): calcd for $C_{20}H_{25}N_3O_4Na$ 394.1737 $[M + Na]^+$; found 394.1726. Anal. Calcd $C_{20}H_{25}N_3O_4$: C, 64.67; H, 6.78; N, 11.31. Found: C, 64.66; H, 6.73; N, 11.11.

4.1.3.2. 4-(tert-Butoxycarbonyl)-1-cinnamoyl-2-methylpiperazine (9). The product was obtained as a solid and purified by column chromatography using hexane–ethyl acetate (2.5:1) as eluent (219 mg, 67% yield), mp 130–133 °C. ^{1}H NMR (500 MHz, DMSO-d_6) δ 7.70 (d, J = 7.0 Hz, 2H), 7.50 (d, J = 15.4 Hz, 1H), 7.46–7.36 (m, 3H), 7.21 (d, J = 15.4 Hz, 1H), 4.73–4.44 (m, 1H), 4.29–3.72 (m, 3H), 3.15–2.73 (m, 3H), 1.43 (s, 9H), 1.13 (bs, 3H). ^{13}C NMR (125 MHz, DMSO-d_6) δ 164.9, 154.3, 141.7, 135.0, 129.6, 128.8, 127.9, 118.3, 79.1, 28.0, 26.8. HRMS (*m/z*): calcd for $C_{19}H_{26}N_2O_3Na$ 353.1836 $[M + Na]^+$; found 353.1830. Anal. Calcd $C_{19}H_{26}N_2O_3$: C, 69.06; H, 7.93; N, 8.48. Found: C, 69.17; H, 7.91; N, 8.40.

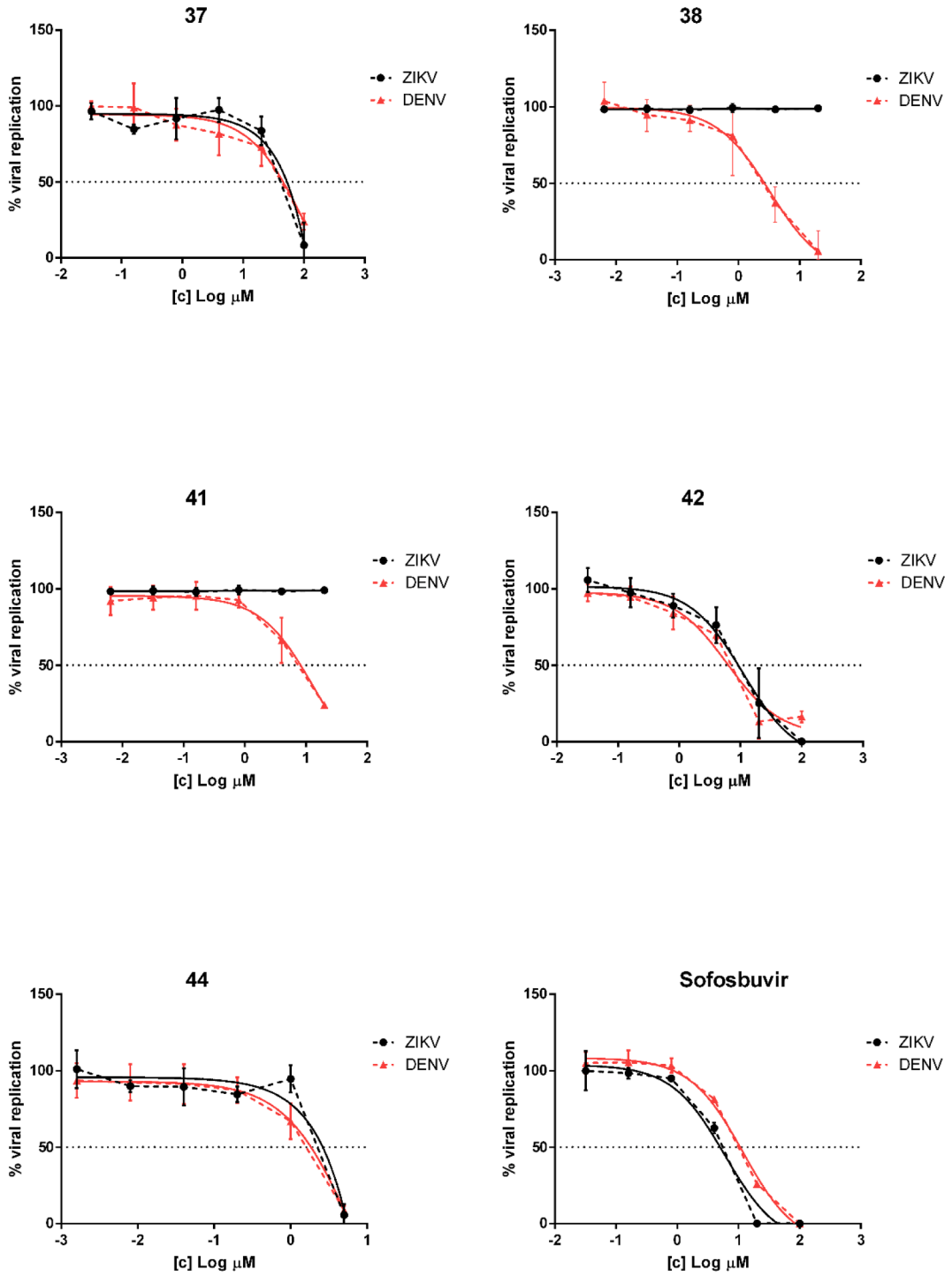

Fig. 4. Inhibitory activity of compound **37**, **38, 41**, **42**, **44** and **sofosbuvir** used as reference compound against ZIKV and DENV in cell culture. The micromolar compound concentration is expressed as logarithm on x-axis, the viral replication is expressed on y-axis as percentage. The normalized curve for each compound derives from 2 independent experiments performed in triplicate.

4.1.3.3. 4-(3,3-Dimethylbutanoyl)-1-[2-(indol-3-yl)-2-oxoacetyl]-2-methylpiperazine (14). The product was obtained as a solid and purified by column chromatography using hexane–ethyl acetate (1:1) as eluent (225 mg, 61% yield), mp 114–118 °C. ^{1}H NMR (500 MHz, DMSO-d_6) δ 12.31 (bs, 1H), 8.25–8.09 (m, 2H), 7.56 (d, J = 7.5 Hz, 1H), 7.34–7.24 (m, 2H), 4.74–4.45 (m, 1H), 4.38–3.76 (m, 3H), 3.13–2.60 (m, 2H), 2.45–1.99 (m, 2H), 1.26–1.08 (m, 3H), 1.05–0.95 (m, 9H). ^{13}C NMR (125 MHz, DMSO-d_6) δ 186.1, 186.0, 170.3, 170.2, 166.0, 137.2, 137.0, 136.9, 124.9, 123.6, 122.6, 120.9, 113.0, 112.7, 50.0, 49.5, 43.6, 43.4, 41.2, 40.6, 40.5, 35.3, 31.0, 29.6, 15.6. 15.4. HRMS (*m/z*): calcd for $C_{21}H_{27}N_3O_3Na$ 392.1945 $[M + Na]^+$; found 392.1933. Anal. Calcd $C_{21}H_{27}N_3O_3$: C, 68.27; H, 7.37; N, 11.37. Found: C, 67.63; H, 7.40; N, 11.30.

4.1.3.4. 1-Cinnamoyl-4-(3,3-dimethylbutanoyl)-2-methylpiperazine (15). The product was obtained as a solid and purified by column chromatography using hexane–ethyl acetate (1:1) as eluent (148 mg, 62% yield), mp 157–160 °C. ^{1}H NMR (500 MHz, DMSO-d_6) δ 7.90–7.10

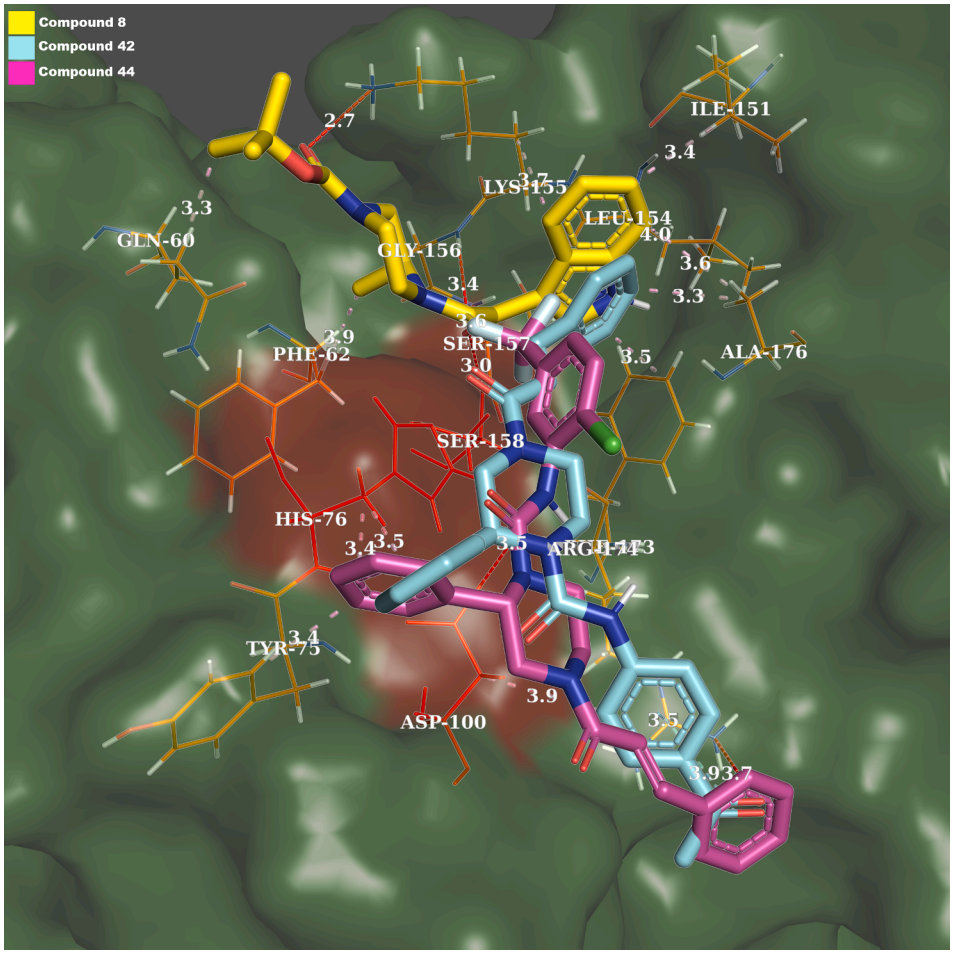

Fig. 5. HCV NS3/4A structure indicating interactions of the three compounds **8**, **42** and **44** with the active site.

(m, 9H), 4.79–4.47 (m, 1H), 4.38–3.74 (m, 3H), 2.95–2.64 (m, 3H), 2.41–1.96 (m, 2H), 1.31–0.76 (m, 12H). ^{13}C NMR (125 MHz, DMSO-d_6) δ 170.3, 170.2, 164.8, 141.7, 135.1, 129.5, 128.7, 128.0, 118.4, 49.5, 45.6, 44.6, 31.0, 30.9, 29.7, 15.6. HRMS (*m/z*): calcd for $C_{20}H_{28}N_2O_2Na$ 351.2043 $[M + Na]^+$; found 351.2032. Anal. Calcd $C_{20}H_{28}N_2O_2$: C, 73.14; H, 8.59; N, 8.53. Found: C, 73.42; H, 8.37; N, 8.24.

4.1.3.5. 4-(tert-Butoxycarbonyl)-1-[2-(indol-3-yl)-2-oxoacetyl]-2-phenylpiperazine (20). The product was obtained as a solid and purified by column chromatography using hexane–ethyl acetate (2:1) as eluent (273 mg, 63% yield), mp 154–156 °C. ^{1}H NMR (500 MHz, DMSO-d_6) δ 12.36 (bs, 1H), 8.33, 8.23 (2 s, 1H), 8.16, 8.11 (dd, J = 7.3 Hz, 1H), 7.57, 7.53 (2d, J = 7.8 Hz, 1H), 7.48–7.21 (m, 8H), 5.71 (m, 1H), 4.96 (m, 1H), 4.58 (d, J = 12.6 Hz, 1H), 4.01–3.46 (m, 2H). 3.20–2.70 (m, 2H), 1.35 (s, 9H). ^{13}C NMR (125 MHz, DMSO-d_6) δ 186.1, 167.3, 137.8, 137.4, 129.1, 128.9, 127.3, 127.1, 125.4, 124.2, 124.1, 123.2, 123.1, 121.5, 121.4, 113.6, 113.2, 79.8, 56.3, 28.4. HRMS (*m/z*): calcd for $C_{25}H_{27}N_3O_4Na$ 456.1894 $[M + Na]^+$; found 456.1897. Anal. Calcd $C_{25}H_{27}N_3O_4$: C, 69.27; H, 6.28; N, 9.69. Found: C, 69.23; H, 6.48; N, 9.39.

4.1.3.6. 4-(tert-Butoxycarbonyl)-1-Cinnamoyl-2-phenylpiperazine (21). The product was obtained as a solid and purified by column chromatography using hexane–ethyl acetate (4:1) as eluent (279 mg, 71% yield), mp 193–196 °C. ^{1}H NMR (500 MHz, DMSO-d_6) δ 7.87–7.26 (m, 12H), 5.84–5.66 (m, 1H), 4.60–4.21 (m, 2H), 3.98–3.72 (m, 2H), 3.32–2.94 (m, 2H), 1.41 (s, 9H). ^{13}C NMR (125 MHz, DMSO-d_6) δ 165.9, 142.9, 135.5, 130.2, 129.3, 128.9, 128.5, 126.9, 118.5, 79.8, 55.4, 28.3. HRMS (*m/z*): calcd for $C_{24}H_{28}N_2O_3Na$ 415.1992 $[M + Na]^+$; found 415.1987.

4.1.3.7. 4-(3,3-Dimethylbutanoyl)-1-[2-(indol-3-yl)-2-oxoacetyl]-2-phenylpiperazine (25). The product was obtained as a solid and purified by column chromatography using hexane–ethyl acetate (2.5:1) as eluent (310 mg, 72% yield), mp 124–126 °C. ^{1}H NMR (500 MHz, DMSO-d_6) δ 12.41 (bs, 1H), 8.43–8.33 (2 s, 1H), 8.24–8.02 (m, 1H), 7.62, 7.58 (2d, J = 7.8 Hz, 1H), 7.51–7.24 (m, 7H), 5.83, 5.64 (2bs, 1H), 5.21–5.02 (m, 1H), 4.54–3.50 (m, 3H), 3.25–2.87 (m, 2H), 2.40–2.01 (m, 2H), 0.92, 0.89 (2 s, 9H). ^{13}C NMR (125 MHz, DMSO-d_6) δ 185.7, 170.3, 166.7, 137.9, 137.5, 129.1, 128.8, 127.9, 127.3, 125.4, 124.3, 123.1, 121.5, 113.6, 113.2, 67.8, 56.6, 51.5, 46.4, 43.6, 31.5, 29.5. HRMS (*m/z*): calcd for $C_{26}H_{29}N_3O_3Na$ 454.2101 $[M + Na]^+$; found 454.2101 Anal. Calcd $C_{26}H_{29}N_3O_3$: C, 72.37; H, 6.77; N, 9.74. Found: C, 71.93; H, 6.74; N, 9.41.

4.1.3.8. 1-(tert-Butoxycarbonyl)-4-[2-(indol-3-yl)-2-oxoacetyl]piperazine (32). The product was obtained as a solid and purified by column chromatography using hexane–ethyl acetate (1:1) as eluent (336 mg, 94% yield), mp 190–192 °C. ^{1}H NMR (500 MHz, DMSO-d_6) δ 12.41 (br s, 1H), 8.20 (d, J = 3.2 Hz, 1H), 8.15–8.12 (m, 1H), 7.57–7.53 (m, 1H), 7.33–7.25 (m, 2H), 3.64–3.59 (m, 2H), 3.51–3.46 (m, 2H), 1.42 (s, 9H). ^{13}C NMR (125 MHz, DMSO-d_6) δ 186.1, 166.1, 153.8, 137.3, 137.0, 124.9, 123.6, 122.6, 121.0, 113.1, 112.6, 79.3, 45.3, 40.5, 28.0. HRMS (*m/z*): calcd for $C_{19}H_{23}N_3O_4Na$ 380.1574 $[M + Na]^+$; found 380.1581. Anal. Calcd $C_{19}H_{23}N_3O_4$: C, 63.85; H, 6.49; N, 11.76. Found: C, 63.44; H, 6.42; N, 11.54.

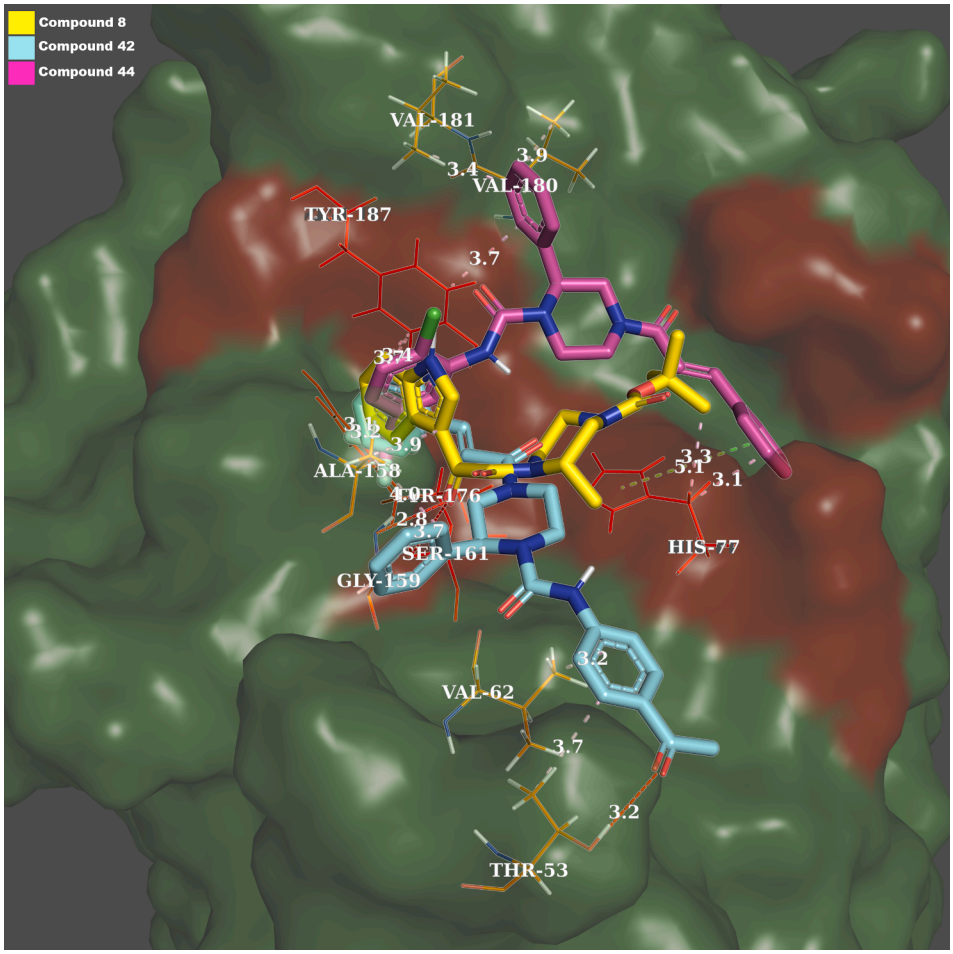

Fig. 6. ZIKV NS3/2B structure indicating interactions of the three compounds **8**, **42** and **44** with the active site.

4.1.3.9. 1-(tert-Butoxycarbonyl)-4-cinnamoylpiperazine (33). The product was obtained as a solid and purified by column chromatography using hexane–ethyl acetate (1.5:1) as eluent (249 mg, 79% yield), mp 139–144 °C. ^{1}H NMR (500 MHz, DMSO-d_6) δ 7.76–7.70 (m, 2H), 7.52 (d, J_{trans} = 15.5 Hz, 1H), 7.45–7.37 (m, 3H), 7.26 (d, J_{trans} = 15.5 Hz, 1H), 3.76–3.52 (m, 4H), 3.44–3.34 (m, 4H), 1.44 (s, 9H). ^{13}C NMR (125 MHz, DMSO-d_6) δ 164.6, 153.8, 141.8, 135.0, 129.6, 128.7, 128.0, 118.3, 79.4, 44.8, 41.4, 28.0. HRMS (*m/z*): calcd for $C_{18}H_{24}N_2O_3Na$ 339.1679 $[M + Na]^+$; found 339.1675. Anal. Calcd $C_{18}H_{24}N_2O_3$: C, 68.33; H, 7.65; N, 8.85. Found: C, 67.95; H, 7.54; N, 8.76.

(B) By reaction with carboxylic acid: To a solution of the appropriate carboxylic acid (1.3 mmol) in dry DMF (10 mL) EDCI (1.5 mmol), and HOBt (1.7 mmol) were added and stirred at room temperature for 45 min. Then a solution of the monoamide (1.0 mmol) in dry DMF (15 mL) was added. The reaction mixture was stirred at room temperature for 72 h until TLC showed that all the starting material had reacted. The reaction mixture was diluted (ethyl acetate, 10 mL) and successively washed with diluted aqueous saturated solution of sodium bicarbonate, brine and dried (Na_2SO_4), filtered and the filtrate was evaporated to dryness. The compounds obtained were purified by flash chromatography on silica gel.

4.1.3.10. 4-(tert-Butoxycarbonyl)-2-methyl-1-(quinoline-3-carbonyl) piperazine (10). The product was obtained as an oil and purified by column chromatography using ethyl acetate–methanol (40:1) as eluent (333 mg, 94% yield). ^{1}H NMR (500 MHz, DMSO-d_6) δ 8.94 (s, 1H), 8.46 (s, 1H), 8.07 (m, 2H), 7.84 (m, 1H), 7.67 (m, 1H), 4.72 (m, 1H), 4.16–3.64 (m, 3H), 3.28–2.84 (m, 3H), 1.41 (s, 9H), 1.21 (m, 3H). ^{13}C NMR (125 MHz, DMSO-d_6) δ 167.1, 154.2, 148.3, 147.5, 134.2, 130.6, 129.1, 128.7, 128.6, 127.3, 126.6, 79.0, 48.0, 46.7, 43.6, 42.8, 27.9, 15.2. HRMS (*m/z*): calcd for $C_{20}H_{26}N_3O_3$ 356.1969 $[M + H]^+$; found 356.1964. Anal. Calcd $C_{20}H_{25}N_3O_3$: C, 67.58.; H, 7.09; N, 11.82. Found: C, 67.81; H, 7.12; N, 11.74.

4.1.3.11. 4-(3,3-Dimethylbutanoyl)-2-methyl-1-(quinoline-3-carbonyl) piperazine (16). The product was obtained as an oil and purified by column chromatography using ethyl acetate–methanol (40:1) as eluent (311 mg, 88% yield). ^{1}H NMR (500 MHz, DMSO-d_6) δ 8.94 (d, J = 1.8 Hz, 1H), 8.48 (s, J = 1.8 Hz 1H), 8.10 (s, 1H), 8.08 (s, 1H), 7.89–7.84 (m, 1H), 7.73–7.67 (m, 1H), 4.39–4.26 (m, 1H), 4.41–4.20 (m, 1H), 4.13–3.79 (m, 2H), 3.45–3.37 (m, 1H), 3.26–3.15 (m, 1H), 2.98–2.72 (m, 1H), 2.44–2.05 (m, 2H), 1.23, 1.16 (2d, J = 5.1 Hz, 3H), 1.02, 1.01 (2 s, 9H). ^{13}C NMR (125 MHz, DMSO-d_6) δ 170.3, 167.1, 148.3, 147.5, 134.3, 130.6, 129.1, 128.7, 128.6, 127.4, 126.6, 45.8, 43.6, 43.4, 31.0, 30.9, 29.7, 28.4, 15.5. HRMS (*m/z*): calcd for $C_{21}H_{28}N_3O_2$ 354.2176 $[M + H]^+$; found 354.2170. Anal. Calcd $C_{21}H_{27}N_3O_3$: C, 71.36; H, 7.70; N, 11.89. Found: C, 71.07; H, 7.81; N, 11.69.

4.1.3.12. 4-(tert-Butoxycarbonyl)-2-phenyl-1-(quinoline-3-carbonyl) piperazine (22). The product was obtained as an oil and purified by column chromatography using hexane–ethyl acetate (2.5:1) as eluent (376 mg, 90% yield). ^{1}H NMR (500 MHz, DMSO-d_6) δ 9.03 (s, 1H), 8.61 (s, 1H), 8.17–8.06 (m, 2H), 7.89 (t, J = 7.6 Hz, 1H,) 7.73 (t, J = 7.4 Hz, 1H), 7–55–7.29 (m, 5H), 5.98–5.65 (m, 1H), 4.69–4.49 (m, 1H), 4.00–3.66 (m, 3H), 3.34–3.01 (m, 2H), 1.38 (s, 9H). ^{13}C NMR (125 MHz, DMSO-d_6) δ 168.7, 154.0, 148.0, 135.1, 131.3, 129.3, 129.2, 129.0, 127.9, 127.6, 127.1, 79.7, 60.3, 46.5, 42.9, 28.3. HRMS (*m/z*): calcd for

$C_{25}H_{28}N_3O_3$ 418.2125 $[M + H]^+$; found 418.2123.

4.1.3.13. 4-(3,3-Dimethylbutanoyl)-2-phenyl-1-(quinoline-3-carbonyl) piperazine (26). The product was obtained as an oil and purified by column chromatography using hexane–ethyl acetate (1:1) as eluent (328 mg, 79% yield). ^{1}H NMR (500 MHz, DMSO-d_6) δ 9.00 (s, 1H), 8.67 (s, 1H), 8.13–7.98 (m, 2H), 7.90–7.64 (m, 2H), 7.52–7.18 (m, 5H), 6.11–5.47 (m, 1H), 5.12–4.87 (m, 1H), 4.59–3.73 (m, 3H), 3.30–3.03 (m, 2H), 2.35–1.75 (m, 2H), 0.89, 0.83 (2 s, 9H). ^{13}C NMR (125 MHz, DMSO-d_6) δ 170.8, 159.4, 140.0, 148.2, 135.1, 131.4, 129.3, 129.2, 129.1, 127.9, 127.7, 127.0, 70.3, 67.7, 67.6, 46.7, 44.1, 31.5, 30.0. HRMS (*m/z*): calcd for $C_{26}H_{30}N_3O_2$ 416.2333 $[M + H]^+$; found 416.2330.

4.1.3.14. 4-(tert-Butoxycarbonyl)-1-[2-(indol-3-yl)acetyl]-2-methylpiperazine (30). The product was obtained as a solid and purified by column chromatography using hexane–ethyl acetate (2:1) as eluent (264 mg, 74% yield), mp 186–188 °C. ^{1}H NMR (500 MHz, DMSO-d_6) δ 10.89 (s, 1H), 7.55 (d, $J = 7.9$ Hz, 1H), 7.35 (d, $J = 7.9$ Hz, 1H), 7.20 (d, $J = 7.2$ Hz, 1H), 7.07 (t, $J = 7.6$ Hz, 1H), 6.97 (t, $J = 7.4$ Hz, 1H), 4.64–4.15 (m, 2H), 3.96–3.60 (m, 4H), 3.18–2.96 (m, 3H), 1.39 (s, 9H), 0.98 (d, $J = 6.8$ Hz, 3H). ^{13}C NMR (125 MHz, DMSO-d_6) δ 169.8, 154.7, 136.7, 121.5, 118.8, 111.9, 79.5, 48.8, 44.6, 40.8, 35.9, 28.5, 15.2. HRMS (*m/z*): calcd for $C_{20}H_{27}N_3O_3Na$ 380.194 $[M + Na]^+$; found 380.1940.

4.1.3.15. 4-(tert-Butoxycarbonyl-1-[2-(indol-3-yl)acetyl]-2-phenyl-piperazine (31). The product was obtained as a solid and purified by column chromatography using hexane–ethyl acetate (1:1) as eluent (339 mg, 81% yield), mp 151–153 °C. ^{1}H NMR (500 MHz, DMSO-d_6) δ 10.93 (bs, 1H), 7.67–6.90 (m, 11*H*), 5.70–5.33 (bs, 1H), 4.58–3.43 (m, 3H), 3.28–2.94 (m, 2H), 1.32 (s, 9H). ^{13}C NMR (125 MHz, DMSO-d_6) δ 170.5, 136.3, 128.3, 127.1, 123.7, 118.4, 111.3, 107.8, 79.0, 51.2, 31.1, 28.4, 27.8. HRMS (*m/z*): calcd for $C_{25}H_{29}N_3O_3Na$ 442.2101$[M + Na]^+$; found 442.2099.

4.1.3.16. 1-(tert-Butoxycarbonyl-)-4-[2-(indol-3-yl)acetyl]-piperazine (34). The product was obtained as a solid and purified by column chromatography using hexane–ethyl acetate (1:1) as eluent (267 mg, 78% yield), m.p. 193–198 °C. ^{1}H NMR (500 MHz, DMSO-d_6) δ 9. 94 (s, 1H), 7.61 (d, $J = 7.9$ Hz, 1H), 7.39 (d, $J = 7.9$ Hz, 1H), 7.29–7.25 (m, 1H), 7.12 (t, $J = 7.7$ Hz, 1H), 7.02 (t, $J = 7.5$ Hz, 1H), 3.86–3.80 (m, 2H), 3.58–3.46 (m, 4H), 3.33–3.19 (m, 4H), 1.35 (s, 9H). 13C NMR (125 MHz, DMSO-d_6) δ 169.9, 154.3, 136.6, 127.6, 124.0, 121.5, 119.2, 118.8, 111.8, 108.4, 79.6, 45.8, 41.4, 31.3, 28.5. HRMS (ESI) *m/z*: calcd. for $C_{19}H_{25}N_3O_3Na$ 366.1784 $[M + Na]^+$; found 366.1788 Anal. Calcd for $C_{19}H_{25}N_3O_3$: C, 66.45; H, 7.34; N, 12.24. Found: C, 65.28; H, 7.32; N, 12.04.

4.1.4. General procedure 3. Synthesis of the urea derivatives

To a solution of the monoacyl derivative (**3–6**, **35**, **36**, **39** and **40**) (1.0 mmol) in dry dichloromethane (10 mL) was added the appropriate isocyanate (1.2 mmol). The reaction mixture was stirred at room temperature until TLC showed that all the starting material had reacted. The reaction mixture was evaporated to dryness. The compounds were purified by flash chromatography on silica gel using the appropriate eluent.

4.1.4.1. 1-[(4-Acetylphenyl)aminocarbonyl]-4-tert-butoxycarbonyl-2-methylpiperazine (11). The product was obtained as a solid and purified by column chromatography using hexane–ethyl acetate (1:2.5) as eluent (285 mg, 79% yield), mp 170–173 °C. ^{1}H NMR (500 MHz, DMSO-d_6) δ 8.85 (s, 1H), 7.84 (d, $J = 9.0$ Hz, 2H), 7.59 (d, $J = 8.9$ Hz, 2H), 4.35 (br s, 1H), 4.13–4.06 (m, 1H), 3.97–3.69 (m, 3H), 3.19–3.13 (m, 3H), 3.11–2.74 (m, 2H), 1.41 (s, 9H), 1.08 (d, $J = 6.7$ Hz, 3H). ^{13}C NMR (125 MHz, DMSO-d_6) δ 197.1, 154.8, 145.7, 130.8, 129.6, 118.8, 79.9, 49.2, 48.5, 46.9, 44.1, 43.1, 38.8, 31.1, 28.5, 26.7, 15.3. HRMS (*m/z*): calcd for $C_{19}H_{27}N_3O_4Na$ 384.1894 $[M + Na]^+$; found 384.1888. Anal. Calcd $C_{19}H_{27}N_3O_4$: C, 63.14; H, 7.53; N, 11.63. Found: C, 63.32; H, 7.36; N, 11.51.

4.1.4.2. 4-tert-Butoxycarbonyl-1-[(2,4-dimethoxyphenyl)aminocarbonyl]-2-methylpiperazine (12). The product was obtained as a solid and purified by column chromatography using hexane–ethyl acetate (2:1) as eluent (258 mg, 68% yield), mp 88–90 °C. ^{1}H NMR (500 MHz, DMSO-d_6) δ 7.51 (s, 1H), 7.36 (d, $J = 8.6$ Hz, 1H), 6.59 (d, $J = 2.6$ Hz, 1H), 6.4 (dd, $J = 2.6$ Hz, $J = 8.6$ Hz, 1H), 4.27 (bs, 1H), 3.95–3.85 (m, 1H), 3.79 (s, 3H), 3.77–3.22 (m, 5H), 3.15–2.75 (m, 3H), 1.44 (s, 9H), 1.10 (d, $J = 6.7$ Hz, 3H). ^{13}C NMR (125 MHz, DMSO-d_6) δ 155.7, 155.4, 154.3, 152.6, 125.2, 121.4, 104.0, 98.7, 78.9, 55.7, 55.2, 46.4, 38.1, 28.0, 14.6. HRMS (*m/z*): calcd for $C_{19}H_{30}N_3O_5$ 380.2180 $[M + H]^+$; found 380.2180. Anal. Calcd $C_{19}H_{29}N_3O_5$: C, 60.14; H, 7.70; N, 11.07. Found: C, 60.28; H, 7.67; N, 10.84.

4.1.4.3. 4-tert-Butoxycarbonyl-2-methyl-1-[(3,4,5-trimethoxyphenyl)aminocarbonyl]piperazine (13). The product was obtained as a solid and purified by column chromatography using hexane–ethyl acetate (1:2.5) as eluent (249 mg, 61% yield), mp 171–173 °C. ^{1}H NMR (500 MHz, DMSO-d_6) δ 8.39 (s, 1H), 6.91 (d, $J = 8.6$ Hz, 1H), 4.33 (bs, 1H), 4.01–3.79 (m, 2H), 3.73 (s, 6H), 3.61 (s, 3H), 3.14–2.69 (m, 3H), 1.43 (s, 9H), 1.09 (d, $J = 6.6$ Hz, 3H). ^{13}C NMR (125 MHz, DMSO-d_6) δ 154.6, 154.2, 152.4, 136.5, 132.4, 97.4, 78.9, 60.1, 55.8, 46.2, 38.0, 28.0, 14.7. HRMS (*m/z*): calcd for $C_{20}H_{31}N_3O_6Na$ 432.2105 $[M + Na]^+$; found 432.2094. Anal. Calcd $C_{20}H_{31}N_3O_6$: C, 58.66; H, 7.63; N, 10.26. Found: C, 58.79; H, 7.46; N, 10.12.

4.1.4.4. 1-[(4-Acetylphenyl)aminocarbonyl]-4-(3,3-dimethylbutanoyl)-2-methylpiperazine (17). The product was obtained as a solid and purified by column chromatography using hexane–ethyl acetate (1:2) as eluent (185 mg, 76% yield), mp 199–203 °C. ^{1}H NMR (500 MHz, DMSO-d_6) δ 9.24, 8.88 (2 s, 1H), 7.93, 7.87 (2d, $J = 8.8$ Hz, 2H), 7.62 (d, $J = 8.4$ Hz, 2H) 4.47–4.20 (m, 2H), 4.05–3.79 (m, 2H), 3.20–3.03 (m, 1H), 2.90–2.68 (m, 1H), 2.44–2.05 (m, 2H), 1.13, 1.06 (2d, $J = 6.5$ Hz, 3H), 1.02, 1.01 (2 s, 9H). ^{13}C NMR (125 MHz, DMSO-d_6) δ 196.4, 170.4, 170.2, 154.2, 145.2, 130.6, 129.6, 129.1, 118.3, 117.4, 49.7, 46.7, 46.6, 45.6, 44.7, 43.6, 43.4, 40.9, 38.5, 31.0, 30.9, 29.7, 26.3, 26.2, 15.2, 14.7. HRMS (*m/z*): calcd for $C_{20}H_{29}N_3O_3Na$ 382.2101 $[M + Na]^+$; found 382.2088. Anal. Calcd $C_{20}H_{29}N_3O_3$: C, 66.83; H, 8.13; N, 11.69. Found: C, 66.82; H, 7.91; N, 11.53.

4.1.4.5. 1-[(2,4-Dimethoxyphenyl)aminocarbonyl]-4-(3,3-dimethylbutanoyl)-2-methylpiperazine (18). The product was obtained as a solid and purified by column chromatography using hexane–ethyl acetate (1:2) as eluent (290 mg, 77% yield), mp 112–117 °C. ^{1}H NMR (500 MHz, DMSO-d_6) δ 7.53 (s, 1H), 7.34 (d, $J = 8.5$ Hz, 1H), 6.58 (s, 1H), 6.46 (d, $J = 8.0$ Hz, 1H), 4.34–4.18 (m, 2H), 4.03–3.90 (m, 1H), 3.78 (s, 3H), 3.75 (s, 3H), 3.17–2.64 (m, 3H), 2.44–2.03 (m, 2H), 1.11, 1.05 (2d, $J = 6.5$ Hz, 3H), 1.02, 1.01 (2 s, 9H). ^{13}C NMR (125 MHz, DMSO-d_6) δ 170.3, 170.2, 156.7, 155.4, 152.7, 125.3, 121.3, 104.0, 98.7, 78.9, 55.7, 55.3, 49.7, 46.8, 46.6, 45.7, 44.7, 43.6, 43.4, 40.9, 38.2, 31.0, 30.9, 29.7, 14.9, 14.5. HRMS (*m/z*): calcd for $C_{20}H_{31}N_3O_4Na$ 400.2207 $[M + H]^+$; found 400.2195. Anal. Calcd $C_{20}H_{31}N_3O_4$: C, 63.64; H, 8.28; N, 11.13. Found: C, 64.05; H, 8.16; N, 10.94.

4.1.4.6. 4-(3,3-Dimethylbutanoyl)-2-methyl-1-[(3,4,5-trimethoxyphenyl) aminocarbonyl]piperazine (19). The product was obtained as a solid and purified by column chromatography using hexane–ethyl acetate (1:2) as eluent (275 mg, 68% yield), mp 159–163 °C. ^{1}H NMR (500 MHz, DMSO-d_6) δ 8.37 (s, 1H), 6.88 (s, 2H), 4.42–4.19 (m, 2H), 4.02–3.80 (m, 2H), 3.73 (s, 6H), 3.61 (s, 3H), 3.18–2.96 (m, 2H), 2.89–2.65 (m, 1H), 2.44–2.04 (m, 2H), 1.16–0.90 (m, 12H). ^{13}C NMR (125 MHz, DMSO-d_6)

δ 170.4, 170.2, 154.6, 152.4, 136.5, 132.5, 97.5, 60.1, 49.7, 55.7, 49.7, 46.6, 45.7, 44.7, 43.6, 43.4, 40.95, 38.6, 38.3, 31.0, 30.9, 29.7, 15.1, 14.7. HRMS (*m/z*): calcd for $C_{21}H_{33}N_3O_5Na$ 430.2312 $[M + Na]^+$; found 430.2299. Anal. Calcd $C_{21}H_{33}N_3O_5$: C, 61.90; H, 8.16; N, 10.31. Found: C, 62.27; H, 8.09; N, 10.08.

4.1.4.7. 4-tert-Butoxycarbonyl-1-[(2,4-dimethoxyphenyl)aminocarbonyl]-2-phenylpiperazine (23). The product was obtained as a solid and purified by column chromatography using hexane–ethyl acetate (1.5:1) as eluent (368 mg, 83% yield), mp 144–146 °C. ^{1}H NMR (500 MHz, DMSO-d_6) δ 8.46 (s, 1H), 7.88 (d, J = 8.8 Hz, 1H), 7.55–7.23 (m, 3H), 6.62–6.54 (m, 2H), 6.49–6.44 (m, 2H), 5.34–5.27 (m, 1H), 4.40–4.11 (m, 1H), 4.03–3.91 (m, 1H), 3.74 (s, 3H), 3.70 (s, 3H), 3.52–3.44 (m, 1H), 3.27–3.18 (m, 2H), 3.12–2.97 (m, 1H), 1.32 (bs, 9H). ^{13}C NMR (125 MHz, DMSO-d_6) δ 155.1, 153.3, 149.5, 128.4, 126.6, 122.2, 121.5, 120.5, 104.2, 99.0, 55.72, 55.62, 46.5, 27.9. HRMS (*m/z*): calcd for $C_{24}H_{31}N_3O_5Na$ 464.2156[M + Na]$^+$; found 464.2149.

4.1.4.8. 4-tert-Butoxycarbonyl-2-phenyl-1-[(3,4,5-trimethoxyphenyl)aminocarbonyl]piperazine (24). The product was obtained as a solid and purified by column chromatography using hexane–ethyl acetate (1:1) as eluent (324 mg, 69% yield), mp 79–81 °C. ^{1}H NMR (500 MHz, DMSO-d_6) δ 8.54 (s, 1H), 7.44–7.26 (m, 5H), 6.93 (s, 2H), 4.67 (bs, 1H), 4.53–4.36 (m, 1H), 4.07–3.77 (m, 2H), 3.73 (s, 6H), 3.62 (s, 3H), 3.44–3.33 (m, 1H), 3.15–2.75 (m, 2H), 1.42, 1.35 (2 s, 9H). ^{13}C NMR (125 MHz, DMSO-d_6) δ 154.9, 154.0, 152.4, 136.7, 132.8, 128.4, 128.2, 127.9, 126.3, 97.4, 70.9, 60.3, 55.8, 30.8, 28.2, 27.9. HRMS (*m/z*): calcd for $C_{25}H_{33}N_3O_6Na$ 494.2262[M + Na]$^+$; found 464.2256. Anal. Calcd $C_{25}H_{33}N_3O_6$: C, 63.68; H, 7.05; N, 8.91. Found: C, 63.84; H, 7.24; N, 8.81.

4.1.4.9. 1-[(4-Acetylphenyl)aminocarbonyl]-4-(3,3-dimethylbutanoyl)-2-phenylpiperazine (27). The product was obtained as a solid and purified by column chromatography using hexane–ethyl acetate (1:2) as eluent (384 mg, 91% yield), mp 185–189 °C. ^{1}H NMR (500 MHz, DMSO-d_6) δ 9.08, 8.96 (2 s, 1H), 7.92–7.82 (m, 2H), 7.68–7.55 (m, 2H), 7.41–7.21 (m, 5H), 5.59–5.41 (m, 1H), 4.97–4.83 (m, 1H), 4.33–3.72 (m, 2H), 3.26–3.00 (m, 2H), 2.33–1.81 (m, 2H), 0.91, 0.86 (2 s, 9H). ^{13}C NMR (125 MHz, DMSO-d_6) δ 196.7, 170.1, 154.6, 145.2, 138.9, 130.5, 129.2, 128.4, 127.0, 126.4, 118.4, 53.5, 45.6, 43.7, 43.4, 42.3, 41.2, 30.9, 29.6, 26.3. HRMS (*m/z*): calcd for $C_{25}H_{31}N_3O_3Na$ 444.2258 $[M + Na]^+$; found 444.2252 Anal. Calcd $C_{25}H_{31}N_3O_3$: C, 71.23; H, 7.41; N, 9.97. Found: C, 71.20; H, 7.40; N, 9.46.

4.1.4.10. 1-[(2,4-Dimethoxyphenyl)aminocarbonyl]-4-(3,3-dimethylbutanoyl)-2-phenylpiperazine (28). The product was obtained as a solid and purified by column chromatography using hexane–ethyl acetate (1.5:1) as eluent (315 mg, 72% yield), mp 151–153 °C. ^{1}H NMR (500 MHz, DMSO-d_6) δ 7.63–7.27 (m, 7H), 6.63–6.45 (m, 2H), 5.44–5.23 (m, 1H), 4.79–4.67 (m, 1H), 4.20–3.83 (m, 3H), 3.78, 3.76, 3.70 (3 s, 6H), 3.65–3.56 (m, 1H), 3.32–3.17 (m, 1H), 2.33–1.86 (m 2H), 0.94, 0.92 (2 s, 9H). ^{13}C NMR (125 MHz, DMSO-d_6) δ 170.7, 170,5, 157.1, 156.6, 152.8, 151.7, 140.5, 139.8, 129.0, 128.9, 127.1, 125.0, 123.4, 121.9, 104.5, 99.3, 56.3, 56.1, 55.7, 54.9, 49.1, 46.1, 44.2, 43.9, 43.1, 42.3, 31.4, 31.2, 30.0. HRMS (*m/z*): calcd for $C_{25}H_{33}N_3O_6Na$ 462.2363 [M + Na]$^+$; found 462.2362.

4.1.4.11. 4-(3,3-Dimethylbutanoyl)-2-phenyl-1-[(3,4,5-trimethoxyphenyl)aminocarbonyl]piperazine (29). The product was obtained as a solid and purified by column chromatography using hexane–ethyl acetate (1:10) as eluent (304 mg, 65% yield), mp 158–160 °C. ^{1}H NMR (500 MHz, DMSO-d_6) δ 8.58, 8.47 (2 s, 1H), 7.40–7.22 (m, 5H), 6.94, 6.88 (2 s, 2H), 5.57–5.38 (m, 1H), 5.00–4.25 (m, 1H), 4.08–43.83 (m, 2H), 3.73, 3.71 (2 s, 6H), 3.61, 3.59 (2 s, 3H), 3.31–2.95 (m, 3H), 2.30–1.83 (m 2H), 0.91, 0.86 (2 s, 9H). ^{13}C NMR (125 MHz, DMSO-d_6) δ 171.3, 155.9, 140.3, 137.6, 133.8, 129.6, 128.2, 127.6, 98.6, 61.3, 56.9, 54.7, 46.9, 44.9, 43.6, 32.2, 31.9, 30.8. HRMS (*m/z*): calcd for $C_{26}H_{35}N_3O_5Na$ 492.2469 $[M + Na]^+$; found 492.2462. Anal. Calcd $C_{26}H_{35}N_3O_5$: C, 66.50; H, 7.51; N, 8.95. Found: C, 66.72, H, 7.19; N, 8.67.

4.1.4.12. 4-[(2,4-Dimethoxyphenyl)aminocarbonyl]-1-[2-(indol-3-yl)-2-oxoacetyl]-2-methylpiperazina (37). The product was obtained as a solid and purified by column chromatography using hexane–ethyl acetate (1:10) as eluent (306 mg, 68% yield), mp 169–171 °C. ^{1}H NMR (500 MHz, DMSO-d_6) δ 12.35, 12.33 (2bs, 1H), 8.30–8.16 (m, 2H), 7.71–7.59 (m, 2H), 7.42–7.28 (m, 3H), 6.64–6.61 (m, 1H), 6.52–6.48 (m, 1H), 4.74–4.67 (m, 1H), 4.38–4.18 (m, 1H), 4.09–3.87 (m, 2H), 3.81, 3.80 (2 s, 3H), 3.78 (s, 3H), 3.34–2.87 (m, 2H), 1.32, 1.27 (2d, J = 6.8 Hz, 3H). ^{13}C NMR (125 MHz, DMSO-d_6) δ 186.7, 186.6, 166.5, 166.4, 157.5, 157.4, 156.4, 156.3, 153.6, 153.5, 137.7, 137.5, 137.4, 129.4, 128.7, 126.3, 126.3, 125.4, 124.1, 123.1, 121.7, 121.6, 121.4, 113.6, 113.5, 113.2, 104.5, 99.2, 56.1, 56.0, 55.7, 50.1, 48.5, 47.6, 45.0, 44.2, 43.8, 41.3, 36.0, 16.4, 15.4. HRMS (*m/z*): calcd for $C_{24}H_{26}N_4O_5Na$ 473.1801 [M + Na]$^+$; found 473.1787.

4.1.4.13. 4-[(2,4-Dimethoxyphenyl)aminocarbonyl-1-[2-(indol-3-yl)-2-oxoacetyl]-]-2-phenylpiperazina (38). The product was obtained as a solid and purified by column chromatography using hexane–ethyl acetate (1:2) as eluent (358 mg, 70% yield), mp 192–195 °C. ^{1}H NMR (500 MHz, DMSO-d_6) δ 12.40 (bs, 1H), 8.37, 8.26 (2 s, 1H), 8.22–8.13 (m, 1H), 7.72–7.25 (m, 10*H*), 6.63–6.44 (m, 2H), 5.74, 5.03 (2 m, 1H), 4.72–3.53 (m, 4H), 3.78 (s, 3H), 3.76 (s, 3H), 3.36–2.90 (m, 2H). ^{13}C NMR (125 MHz, DMSO-d_6) δ 186.3, 167.3, 157.4, 157.3, 155.9, 153.4, 153.3, 138.6, 137.5, 129.2, 128.9, 127.8, 127.4, 127.2, 126.1, 126.0, 125.4, 124.2, 123.2, 123.1, 121.5, 113.6, 113.2, 104.5, 99.2, 56.4, 56.1, 55.7, 51.9, 45.9, 45.1, 44.2, 43.6, 42.2, 37.2. HRMS (*m/z*): calcd for $C_{29}H_{28}N_4O_5Na$ 535.1957 $[M + Na]^+$; found 535.1944.

4.1.4.14. 1-[(Acetylphenyl)aminocarbonyl]-4-[2-(indol-3-yl)-2-oxoacetyl]-2-phenylpiperazine (41). The product was obtained as a solid and purified by column chromatography using hexane–ethyl acetate (1:2) as eluent (448 mg, 81% yield), mp 182–184 °C. ^{1}H NMR (500 MHz, DMSO-d_6) δ 12.24, 12.17 (2d, J = 2.1 Hz, 1H), 9.14, 9.05 (2 s, 1H), 8.18–7.06 (m, 14H), 5.76 (bs, 1H), 5.08–5.02 (m, 1H), 4.30–4.01 (m, 3H), 3.61–3.35 (m, 2H), 3.32 (s, 3H). ^{13}C NMR (125 MHz, DMSO-d_6) δ 196.3, 185.6, 185.4, 166.6, 166.1, 154.7, 154.5, 145.1, 138.7, 138.2, 136.8, 136.3, 130.6, 130.5, 129.2, 129.1, 128.1, 126.9, 126.6, 126.3, 124.9, 124.7, 123.6, 123.5, 122.6, 122.5, 120.9, 120.8, 118.4, 118.3, 113.1, 112.6, 112.5, 59.7, 53.7, 53.2, 47.8, 45.1, 42.4, 40.9, 38.1, 26.3. HRMS (*m/z*): calcd for $C_{29}H_{26}N_4O_4Na$ 517.1846 $[M + Na]^+$; found 517.1834.

4.1.4.15. 1-[(Acetylphenyl)aminocarbonyl]-4-cinnamoyl-2-phenylpiperazina (42). The product was obtained as a solid and purified by column chromatography using dichloromethane-methanol (20:1) as eluent (439 mg, 97% yield), mp 163–165 °C. ^{1}H NMR (500 MHz, DMSO-d_6) δ 9.12, 9.06 (2 s, 1H), 7.92–7.17 (m, 16H), 5.67–5.55 (m, 1H), 5.00–4.72 (m, 1H), 4.29–3.86 (m, 3H), 3.50–3.37 (m, 1H), 3.34 (m, 3H), 3.24–3.15 (m, 1H). ^{13}C NMR (125 MHz, DMSO-d_6) δ 169.4, 154.5, 145.1 141.9, 141.7, 139.9, 135.0, 130.5, 129.6, 129.2, 128.7, 128.5, 128.1, 127.0, 118.4, 117.8, 117.6, 54.2, 53.6, 47.5, 44.6, 43.1, 41.8, 26.3. HRMS (*m/z*): calcd for $C_{28}H_{27}N_3O_3Na$ 476.1945 $[M + Na]^+$; found 476.1935.

4.1.4.16. 1-[(2-Chloro-5-trifluoromethylphenyl)aminocarbonyl]-4-[2-(indol-3-yl)-2-oxoacetyl]-2-phenylpiperazine (43). The product was obtained as a solid and purified by column chromatography using hexane–ethyl acetate (1:1) as eluent (415 mg, 75% yield), mp 190–192 °C. ^{1}H NMR (500 MHz, DMSO-d_6) δ 12.26, 12.17 (2d, J = 2.1 Hz, 1H), 8.62 (s, 1H), 8.30–7.10 (m, 13H), 5.68 (bs, 1H), 5.07–4.96 (m, 1H),

4.24–3.81 (m, 2H), 3.73–3.40 (m, 2H); 3.11–3.01 (m, 1H). ^{13}C NMR (125 MHz, DMSO-d_6) δ 185.6, 185.3, 166.7, 166.2, 154.7, 154.5, 145.1, 138.5, 138.1, 137.5, 137.3, 136.8, 136.4, 130.5, 130.4, 128.7, 128.3, 127.4, 127.3, 126.7, 126.3, 124.9, 124.7, 123.6, 123.5, 122.6, 122.5, 120.9, 120.8, 113.0, 112.6, 112.5, 54.8, 53.7, 47.9, 44.9, 42.5, 41.2, 36.2, 28.2, 24.2. HRMS (*m/z*): calcd for $C_{28}H_{22}ClF_3N_4O_3Na$ 577.1225 $[M + Na]^+$; found 577.1206.

4.1.4.17. 1-[(2-Chloro-5-trifluoromethylphenyl)aminocarbonyl]-4-cinnamoyl-2-phenylpiperazine-1-carboxamida (44) [86]. The product was obtained as a solid and purified by column chromatography using hexane–ethyl acetate (2.5:1) as eluent (477 mg, 93% yield), mp 171–173 °C. ^{1}H NMR (500 MHz, DMSO-d_6) δ 8.46, 8.34 (2 s, 1H), 8.03 (bs, 1H), 7.74–7.67 (m, 3H), 7.56–7.23 (m, 8H), 7.20 (d, J = 15.6 Hz, 1H), 5.57–5.44 (m, 1H), 4.83–4.59 (m, 1H), 4.25–3.95 (m, 3H), 3.62–3.46 (m, 2H). ^{13}C NMR (125 MHz, DMSO-d_6) δ 169.4, 154.6, 141.8, 141.6, 138.9, 137.4, 135.0, 130.4, 129.6, 128.7, 128.6, 128.0, 127.3, 127.0, 126.5, 121.4, 55.2, 54.5, 47.5, 44.6, 43.2, 42.1, 36.2, 28.3, 24.1. HRMS (*m/z*): calcd for $C_{27}H_{23}ClF_3N_3O_3Na$ 536.1326 $[M + Na]^+$; found 536.1308.

4.1.5. General procedure 4. Removal of Boc group

To a solution of the Boc derivatives **8** and **20** (1.0 mmol) in dry dichloromethane (30 mL) was kept into an ice-water up to adding the trifluoroacetic acid (15.0 mmol). The reaction mixture was stirred at room temperature until TLC showed that all the starting material had reacted. The reaction mixture was evaporated to dryness and co-evaporated with toluene. The products **35** and **36** were detected by mass spectrometry and used without purification for the next synthetic step (Section 4.1.4).

4.1.6. General procedure 5. Synthesis of phenyl isocyanate from substituted aniline

According to a published procedure with some modifications [87], to a solution of appropriate substituted aniline (1.87 mmol) in dichloromethane (20 mL) was added an aqueous solution of Na_2CO_3 (3.0 mmol, 20 mL) and the heterogeneous mixture was vigorously stirred for 5 min at rt. Triphosgene (0.62 mmol) was added to the flask and stirred for 30 min. The phases were manually separated, and the organic layer was dried (Na_2SO_4), filtered and evaporated to dryness. The isocyanate was used without further purification in reaction of urea formation.

4.1.6.1. 3,4,5-Trimethoxyphenyl isocyanate. The product was obtained as a pure solid (339 mg, 86% yield). ^{1}H NMR (500 MHz, DMSO-d_6) δ 6.79 (s, 2H, Ar), 3.77 (s, 6H, OCH_3), 3.63 (s, 3H, OCH_3). ^{13}C NMR (125 MHz, DMSO-d_6) δ 152.8, 135.7, 132.6, 96.2, 91.6, 60.0, 55.4. HRMS (*m/z*): calcd for $C_{10}H_{11}NO_4Na$ 210.0761 $[M + Na]^+$; found 210.0757.

4.2. Biology

4.2.1. Hepatitis C virus NS3/4A protease inhibition assay

The HCV NS3/4A protease is required for the cleavage of the viral polyprotein at the NS3-NS4A, NS4A-NS4B, NS4B-NS5A, and NS5A-NS5B sites [88,89]. These proteolytic cleavages are essential for the maturation of the viral proteins in the HCV replicative cycle. Thus, NS3/4A has become one of the key targets for developing anti-HCV drugs [90] and, consequently, was selected as the main target of this study.

We performed the screening assay in the Biology Service of CITIUS at the University of Seville using a microplate reader (Synergy Biotek, VT, USA) and SensoLyte® 520 HCV Protease Assay Kit (Cat#AS-71145; AnaSpec®, Fremont CA, USA), in addition to HCV-genotype 1b NS3/4A protease (Cat#61017; AnaSpec®, Fremont CA, USA). Briefly, the quantification of HCV NS3/4A protease activity was based on the 5-FAM/QXL™520 fluorescence resonance energy transfer (FRET) peptide (tested with the protease assay kit), whose sequence is derived from the cleavage site of NS4A/NS4B. In the FRET peptide, the fluorescence of 5-FAM is quenched by QXL™520. However, upon cleavage into two separate fragments by HCV NS3/4A protease, the fluorescence of 5-FAM is recovered and can be monitored at excitation (490 nm)/emission (520 nm). In addition, the assay can detect as low as 1.56 ng/mL active HCV NS3/4A protease [91]. Therefore, this proteolytic mechanism allows us to relate the protease activity acting on the FRET peptide with the fluorescence intensity.

The assay-related working solutions and the samples were prepared immediately before the screening according to the manufacturer's recommendations. The test compounds were dissolved at 5 mM in dimethyl sulfoxide (DMSO) to obtain a final concentration of 0.5 mM by well, similar to the reference control with Telaprevir (TPV). All measurements were made in triplicate for each compound.

The controls and test compounds were added into each well on a 96-well black microplate (Costar® 96-Well Black Polystyrene Plate) following the protocol previously published [92]: 19 μL of buffer assay, 1 μL of HCV NS3/4A protease, and 5 μL of screening inhibitors, incubated at room temperature for 15 min in the dark. The enzymatic reaction started by adding 25 μL of HCV NS3/4A protease substrate. Immediately, the fluorescence on kinetic mode was recorded at 37C in the microplate reader at λex/em = 490/520 nm every 5 min for 1 h by soft shaking before reading.

The fluorescence reading from the substrate control well is the background fluorescence. The relative fluorescence unit (RFU) was obtained from the readings of the other wells subtracting this background. The reader of fluorescence generated a plot data as RFU versus time for controls and samples. The slope of the RFU curves was determined from the average of the duplicates. Percentage protease inhibition was calculated using the following equation: % inhibition = (slope E + S – slope test compound/ slope E + S) × 100, where the slope E + S is the fluorescence of the enzyme and substrate without Telaprevir, and the slope test compound is the fluorescence of the assay mixture with the potential inhibitors added [93]. Graphs of the percentage of enzymatic activity inhibition of positive, negative, vehicle controls and compounds were generated with GraphPad PRISM software version 9.0.0. (Supplementary information, Fig. S31).

4.2.2. In vitro antiviral activity against Zika and Dengue viruses

Viruses, cells and reference compound.

The H/PF/2013 ZIKV strain, belonging to the Asian lineage, and the New Guinea C DENV serotype 2 strain were kindly provided by the Instituto Superiore di Sanità, Rome, Italy. Once expanded, viral stocks were stored at −80 °C and titrated by plaque assay, as previously described [68].

Vero E6 (African green monkey kidney cell line; ATCC, Manassas, VA, USA, CRL-1586) and C6/36 (Aedes albopictus mosquito; ATCC CRL-1660) cell lines were used to expand ZIKV and DENV, respectively. The *in vitro* cytotoxicity and antiviral activity of candidate compounds was determined in Huh7 cell line (human hepatoma cell line; kindly provided by Instituto Toscano Tumori, Core Research Laboratory, Siena, Italy). Dulbecco's modified Eagle's medium high glucose with sodium pyruvate, and L-glutamine (DMEM High Glucose, Euroclone, Milan, Italy) supplemented with 10% fetal bovine serum (FBS; Euroclone) and 1% of penicillin/streptomycin (Euroclone) was used as propagation medium. The propagation medium was supplemented with 2 mM of L-glutamine and HEPES (25 mM) to propagate the C6/36 medium cell line. The propagation medium with a lower concentration of FBS (1%) was used in infection experiments. The mammalian cells were incubated at 37 °C in a humidified incubator supplemented with 5% CO_2, whereas the mosquito cell line was maintained at 28 °C. Sofosbuvir (MedChem Express cat. HY-15005), used as reference compound, was supplied as a powder, and dissolved in 100% dimethyl sulfoxide (DMSO).

4.2.3. Cytotoxicity assay

Cytotoxicity of compounds was determined by CellTiter-Glo 2.0

Luminescent Cell Viability Assay (Promega) in the Huh7 cell line, according to the manufacturer's protocol. The luminescent signal obtained from cells treated with 5-fold dilution of the test compound, or DMSO as a control, was measured through the GloMax® Discover Microplate Reader (Promega). Raw data were elaborated with the GraphPad PRISM software version 6.01 (La Jolla) to calculate the half-maximal cytotoxic concentration (CC_{50}). The putative inhibitory activity of compounds was tested starting from the concentration causing the 20% of cellular toxicity (CC_{20}).

4.2.4. Antiviral assay

Immunodetection assay (IA) using a pan-flavivirus monoclonal antibody recognizing a conserved domain of the envelope protein was the read out to determine the antiviral activity of candidate compounds on the whole viral replication cycle as previously published [66,67] Briefly, 7,000 Huh7 cells per well were infected using 50 $TCID_{50}$ (50% tissue culture infectious dose $TCID_{50}$) of DENV or ZIKV viral stocks, as defined by previous titration according to Reed & Muench [94]. Viral adsorption was performed in 96-well plates for 1 h at 37 °C with 5% CO_2 and after virus removal, serial dilutions of each compound tested were added to the cells and incubated at 37 °C with 5% CO_2. After 72 h, culture supernatants were collected, properly diluted, and used to re-infect in triplicate uninfected Huh7 cells in absence of the compounds (infectious virus yield) for 72 h at 37 °C with 5% CO_2. After incubation, cells were fixed for 30 min with 10% formaldehyde (Carlo Erba), rinsed with 1% PBS and permeabilized for 10 min with 1% Triton X-100 (Carlo Erba). After washing, cells monolayer was incubated with monoclonal anti-flavivirus mouse antibody (clone D1-4G2-4–15; Novus Bio) and then with a polyclonal Horseradish Peroxidase (HRP)-coupled anti-mouse IgG secondary antibody (Novus Bio NB7570). Absorbance values were measured after 10 min incubations with the 3,3′,5,5′-tetramethylbenzidine substrate (TMB, Sigma Aldrich) and signals were acquired at 450 nm optical density (OD450) using the absorbance module of the GloMax® Discover Multimode Microplate Reader (Promega). Each IA run was validated by the OD450 value above 1 in the virus control culture. All drug concentrations were tested in triplicate in two independent experiments. In each test, sofosbuvir was used as reference compounds and infected and uninfected cells without drugs were used to calculate the 100% and 0% of viral replication, respectively. The half-maximal inhibitory concentration (IC_{50}) was calculated through a non-linear regression analysis of the dose–response curves generated with GraphPad PRISM software version 6.01. Selectivity Index (SI) of compounds was calculated as ratio between CC_{50} and IC_{50}.

4.3. Docking studies

4.3.1. Dataset

Inactive structural conformation for ZIKV and HCV NS3 Proteases were extracted from the X-ray crystal structure chain A in the PDB Database for each protease (PDB ID: 5LC0 [75] and 6PJ1 [73], respectively). After that, we processed the structure files through Maestro (https://www.schrodinger.com) to obtain mol2 files with assigned charges and prepared for the virtual screening technique using OPLS3e as force field and different tools to fill possible missing side or loops, assign bonds and add hydrogens to the structure.

We obtained ligand mol2 files from the generated cdx files through different conversion programs. First, we converted cdx files to smi format via Open Babel [95] converter tool. After that, these smi files were transformed to mol2 files via the Chemaxon tool molconvert to obtain the mol2 files used for molecular modeling.

4.3.2. Molecular modeling

When the ligand and protein structures had been prepared, we carried out a molecular modeling protocol with the Lead Finder [96] docking program to obtain docking scores and details about interactions between protein and generated compounds. These calculations were performed for compounds **8**, **42** and **44** against 5CL0 and 6PJ1 pre-processed structures via the metascreener tool (https://github.com/bio-hpc/metascreener). Thus, we executed calculations via Lead Finder for each protease with the same compounds as queries in an HPC server and in parallel.

Declaration of Competing Interest

The authors declare that they have no known competing financial interests or personal relationships that could have appeared to influence the work reported in this paper.

Data availability

No data was used for the research described in the article.

Acknowledgements

This work has been supported by Ministerio de Ciencia, Innovación y Universidades, Plan Estatal 2017-2020 Retos - Proyectos I + D + i (PID2019-104767RB-I00). MRGL also thanks Ministerio de Economía y Competitividad, Instituto de Salud Carlos III (grants PI19/00589, PI19/01404, PI16/01842, PI17/00535 and GLD19/00100) for financial support.

This work was supported by funds from MIUR Ministero dell'Istruzione, dell'Università della Ricerca Italiano, project PRIN 2017, ORIGINALE CHEMIAE in Antiviral Strategy—Origin and Modernization of Multi-Component Chemistry as a Source of Innovative Broad-Spectrum Antiviral Strategy (cod. 2017BMK8JR) and from Tuscany region, project Tuscany Antiviral Research Network -TUSCAVIR.NET (Bando Ricerca Salute 2018). We would like to thank Giulietta Venturi for making the ZIKV H/PF/2013 strain available for this study.

This work has also been funded by the Fundación Séneca de la Región de Murcia under Project 20988/PI/18.

This research was partially supported by the computer resources and the technical support provided by the supercomputing infrastructure of the NLHPC (ECM-02), Powered@NLHPC and the Extremadura Research Centre for Advanced Technologies (CETA − CIEMAT), funded by the European Regional Development Fund (ERDF). CETA − CIEMAT is part of CIEMAT and the Government of Spain.

Authors thank CITIUS (Centro de Investigación, Tecnología e Innovación de la Universidad de Sevilla) for its important contribution in recording NMR and Mass spectra and in elemental analysis determination.

Appendix A. Supplementary material

Supplementary data to this article can be found online at https://doi.org/10.1016/j.bioorg.2023.106408.

References

[1] N. Vasilakis, S.C. Weaver, Flavivirus transmission focusing on Zika, Curr. Opin. Virol. 22 (2017) 30–35, https://doi.org/10.1016/j.coviro.2016.11.007.
[2] N. Alzahrani, M.J. Wu, S. Shanmugam, M.K. Yi, Delayed by design: Role of suboptimal signal peptidase processing of viral structural protein precursors in flaviviridae virus assembly, Viruses. 12 (2020), https://doi.org/10.3390/v12101090.
[3] Z. Weng, X. Shao, D. Graf, C. Wang, C.D. Klein, J. Wang, G.C. Zhou, Identification of fused bicyclic derivatives of pyrrolidine and imidazolidinone as dengue virus-2 NS2B-NS3 protease inhibitors, Eur. J. Med. Chem. 125 (2017) 751–759, https://doi.org/10.1016/j.ejmech.2016.09.063.
[4] T.C. Pierson, M.S. Diamond, The continued threat of emerging flaviviruses, Nat. Microbiol. 5 (2020) 796–812, https://doi.org/10.1038/s41564-020-0714-0.
[5] S. Nie, Y. Yao, F. Wu, X. Wu, J. Zhao, Y. Hua, J. Wu, T. Huo, Y.L. Lin, A. R. Kneubehl, M.B. Vogt, J. Ferreon, R. Rico-Hesse, Y. Song, Synthesis, structure-activity relationships, and antiviral activity of allosteric inhibitors of flavivirus NS2B-NS3 protease, J. Med. Chem. 64 (2021) 2777–2800, https://doi.org/10.1021/acs.jmedchem.0c02070.

[6] F. Roudot-Thoraval, Epidemiology of hepatitis C virus infection, Clin. Res. Hepatol. Gastroenterol. 45 (2021) 2015–2020, https://doi.org/10.1016/j.clinre.2020.101596.

[7] WHO 2022: Hepatitis C (2022) 2022. <https://www.who.int/news-room/fact-sheets/detail/hepatitis-c> (Accessed: 2022-11-11).

[8] M.S. Mehand, F. Al-Shorbaji, P. Millett, B. Murgue, The WHO R&D Blueprint: 2018 review of emerging infectious diseases requiring urgent research and development efforts, Antiviral Res 159 (2018) 63–67, https://doi.org/10.1016/j.antiviral.2018.09.009.

[9] WHO 2022: Dengue and severe dengue (2022) 2022. <https://www.who.int/news-room/fact-sheets/detail/dengue-and- severe-dengue> (Accessed: 2022-11-11).

[10] H. Harapan, A. Michie, R.T. Sasmono, A. Imrie, Dengue: a minireview, Viruses. 12 (2020) 1–35, https://doi.org/10.3390/v12080829.

[11] A. Wahaab, B.E. Mustafa, M. Hameed, N.J. Stevenson, M.N. Anwar, K. Liu, J. Wei, Y. Qiu, Z. Ma, Potential role of flavivirus NS2B-NS3 proteases in viral pathogenesis and anti-flavivirus drug discovery employing animal cells and models, A Review (2022) 1–27.

[12] H.E. Clapham, B.A. Wills, Implementing a dengue vaccination programme-who, where and how? Trans. R. Soc. Trop. Med. Hyg. 112 (2018) 367–368, https://doi.org/10.1093/trstmh/try070.

[13] M.R. Capeding, N.H. Tran, S.R.S. Hadinegoro, H.I.H.M. Ismail, T. Chotpitayasunondh, M.N. Chua, C.Q. Luong, K. Rusmil, D.N. Wirawan, R. Nallusamy, P. Pitisuttithum, U. Thisyakorn, I.K. Yoon, D. Van Der Vliet, E. Langevin, T. Laot, Y. Hutagalung, C. Frago, M. Boaz, T.A. Wartel, N. G. Tornieporth, M. Saville, A. Bouckenooghe, Clinical efficacy and safety of a novel tetravalent dengue vaccine in healthy children in Asia: a phase 3, randomised, observer-masked, placebo-controlled trial, Lancet. 384 (2014) 1358–1365, https://doi.org/10.1016/S0140-6736(14)61060-6.

[14] S. Spizzichino, G. Mattedi, K. Lauder, C. Valle, W. Aouadi, B. Canard, E. Decroly, S. J.F. Kaptein, J. Neyts, C. Graham, Z. Sule, D.J. Barlow, R. Silvestri, D. Castagnolo, Design, synthesis and discovery of N, N'-carbazoyl-aryl-urea inhibitors of Zika NS5 methyltransferase and virus replication, ChemMedChem. 15 (2020) 385–390, https://doi.org/10.1002/cmdc.201900533.

[15] N. Palanisamy, D. Akaberi, J. Lennerstrand, Protein backbone flexibility pattern is evolutionarily conserved in the Flaviviridae family: A case of NS3 protease in Flavivirus and Hepacivirus, Mol. Phylogenet. Evol. 118 (2018) 58–63, https://doi.org/10.1016/j.ympev.2017.09.015.

[16] S.P. Lim, Q.Y. Wang, C.G. Noble, Y.L. Chen, H. Dong, B. Zou, F. Yokokawa, S. Nilar, P. Smith, D. Beer, J. Lescar, P.Y. Shi, Ten years of dengue drug discovery: progress and prospects, Antiviral Res. 100 (2013) 500–519, https://doi.org/10.1016/j.antiviral.2013.09.013.

[17] N. Pathak, Y.P. Kuo, T.Y. Chang, C.T. Huang, H.C. Hung, J.T.A. Hsu, G.Y. Yu, J. M. Yang, Zika virus NS3 protease pharmacophore anchor model and drug discovery, Sci. Rep. 10 (2020) 1–17, https://doi.org/10.1038/s41598-020-65489-w.

[18] N. Pathak, M.L. Lai, W.Y. Chen, B.W. Hsieh, G.Y. Yu, J.M. Yang, Pharmacophore anchor models of flaviviral NS3 proteases lead to drug repurposing for DENV infection, BMC Bioinform. 18 (2017), https://doi.org/10.1186/s12859-017-1957-5.

[19] H. Lee, J. Ren, S. Nocadello, A.J. Rice, I. Ojeda, S. Light, G. Minasov, J. Vargas, D. Nagarathnam, W.F. Anderson, M.E. Johnson, Identification of novel small molecule inhibitors against NS2B/NS3 serine protease from Zika virus, Antiviral Res. 139 (2017) 49–58, https://doi.org/10.1016/j.antiviral.2016.12.016.

[20] J. Sánchez-Céspedes, P. Martínez-Aguado, M. Vega-Holm, A. Serna-Gallego, J. I. Candela, J.A. Marrugal-Lorenzo, J. Pachón, F. Iglesias-Guerra, J.M. Vega-Pérez, New 4-Acyl-1-phenylaminocarbonyl-2-phenylpiperazine derivatives as potential inhibitors of adenovirus infection. synthesis, biological evaluation, and structure-activity relationships, J. Med. Chem. 59 (2016) 5432–5448, https://doi.org/10.1021/acs.jmedchem.6b00300.

[21] S. Mazzotta, J.A. Marrugal-Lorenzo, M. Vega-Holm, A. Serna-Gallego, J. Álvarez-Vidal, J. Berastegui-Cabrera, J. Pérez del Palacio, C. Díaz, F. Aiello, J. Pachón, F. Iglesias-Guerra, J.M. Vega-Pérez, J. Sánchez-Céspedes, Optimization of piperazine-derived ureas privileged structures for effective antiadenovirus agents, Eur. J. Med. Chem. 185 (2020), https://doi.org/10.1016/j.ejmech.2019.111840.

[22] M. Bassetto, P. Leyssen, J. Neyts, M.M. Yerukhimovich, D.N. Frick, M. Courtney-Smith, A. Brancale, In silico identification, design and synthesis of novel piperazine-based antiviral agents targeting the hepatitis C virus helicase, Eur. J. Med. Chem. 125 (2017) 1115–1131, https://doi.org/10.1016/j.ejmech.2016.10.043.

[23] Y. Wang, R. Zhou, Y. Quan, S. Chen, X. Shi, Y. Li, S. Cen, Design, synthesis, and evaluation of novel 4-amino-2-(4-benzylpiperazin-1-yl)methylbenzonitrile compounds as Zika inhibitors, Bioorg. Med. Chem. Lett. 30 (2020), 126906, https://doi.org/10.1016/j.bmcl.2019.126906.

[24] L. Li, C. Basavannacharya, K.W.K. Chan, L. Shang, S.G. Vasudevan, Z. Yin, Structure-guided discovery of a novel non-peptide inhibitor of dengue virus NS2B-NS3 protease, Chem. Biol. Drug Des. 86 (2015) 255–264, https://doi.org/10.1111/cbdd.12500.

[25] M.X. Dong, L. Lu, H. Li, X. Wang, H. Lu, S. Jiang, Q.Y. Dai, Design, synthesis, and biological activity of novel 1,4-disubstituted piperidine/piperazine derivatives as CCR5 antagonist-based HIV-1 entry inhibitors, Bioorg. Med. Chem. Lett. 22 (2012) 3284–3286, https://doi.org/10.1016/j.bmcl.2012.03.019.

[26] D. Dou, G. He, S.R. Mandadapu, S. Aravapalli, Y. Kim, K.O. Chang, W.C. Groutas, Inhibition of noroviruses by piperazine derivatives, Bioorg. Med. Chem. Lett. 22 (2012) 377–379, https://doi.org/10.1016/j.bmcl.2011.10.122.

[27] X. Zhang, H. Wang, Y. Li, R. Cao, W. Zhong, Z. Zheng, G. Wang, J. Xiao, S. Li, Novel substituted heteroaromatic piperazine and piperidine derivatives as inhibitors of human enterovirus 71 and coxsackievirus A16, Molecules. 18 (2013) 5059–5071, https://doi.org/10.3390/molecules18055059.

[28] M. Shaquiquzzaman, G. Verma, A. Marella, M. Akhter, W. Akhtar, M.F. Khan, S. Tasneem, M.M. Alam, Piperazine scaffold: A remarkable tool in generation of diverse pharmacological agents, Eur. J. Med. Chem. 102 (2015) 487–529, https://doi.org/10.1016/j.ejmech.2015.07.026.

[29] M. Saudi, J. Zmurko, S. Kaptein, J. Rozenski, B. Gadakh, P. Chaltin, A. Marchand, J. Neyts, A. Van Aerschot, Synthetic strategy and antiviral evaluation of diamide containing heterocycles targeting dengue and yellow fever virus, Eur. J. Med. Chem. 121 (2016) 158–168, https://doi.org/10.1016/j.ejmech.2016.05.043.

[30] P. Sikka, Role of aryl urea containing compounds in medicinal chemistry, Med. Chem. (Los. Angeles). 5 (2015) 479–483, https://doi.org/10.4172/2161-0444.1000305.

[31] E.M.F. Muri, M. Gomes, M.G. Albuquerque, E.F.F. Da Cunha, R.B. De Alencastro, J. S. Williamson, O.A.C. Antunes, Pseudo-peptides derived from isomannide as potential inhibitors of serine proteases, Amino Acids. 28 (2005) 413–419, https://doi.org/10.1007/s00726-004-0146-9.

[32] S. Mazzotta, J. Berastegui-Cabrera, G. Carullo, M. Vega-Holm, M. Carretero-Ledesma, L. Mendolia, F. Aiello, F. Iglesias-Guerra, J. Pachón, J.M. Vega-Pérez, J. Sánchez-Céspedes, Serinol-based benzoic acid esters as new scaffolds for the development of adenovirus infection inhibitors: design, synthesis, and in vitro biological evaluation, ACS Infect. Dis. 7 (2021), https://doi.org/10.1021/acsinfecdis.0c00515.

[33] S. Mazzotta, J. Berastegui-Cabrera, M. Vega-Holm, M. del R. García-Lozano, M. Carretero-Ledesma, F. Aiello, J.M. Vega-Pérez, J. Pachón, F. Iglesias-Guerra, J. Sánchez-Céspedes, Design, synthesis and in vitro biological evaluation of a novel class of anti-adenovirus agents based on 3-amino-1,2-propanediol, Bioorg. Chem. 114 (2021), https://doi.org/10.1016/j.bioorg.2021.105095.

[34] A.K. Timiri, B.N. Sinha, V. Jayaprakash, Progress and prospects on DENV protease inhibitors, Eur. J. Med. Chem. 117 (2016) 125–143, https://doi.org/10.1016/j.ejmech.2016.04.008.

[35] C. Steuer, C. Gege, W. Fischl, K.H. Heinonen, R. Bartenschlager, C.D. Klein, Synthesis and biological evaluation of α-ketoamides as inhibitors of the Dengue virus protease with antiviral activity in cell-culture, Bioorg. Med. Chem. 19 (2011) 4067–4074, https://doi.org/10.1016/j.bmc.2011.05.015.

[36] M. Robello, E. Barresi, E. Baglini, S. Salerno, S. Taliani, F. Da Settimo, The alpha keto amide moiety as a privileged motif in medicinal chemistry: current insights and emerging opportunities, J. Med. Chem. 64 (2021) 3508–3545, https://doi.org/10.1021/acs.jmedchem.0c01808.

[37] A. Kling, K. Jantos, H. Mack, W. Hornberger, K. Drescher, V. Nimmrich, A. Relo, K. Wicke, C.W. Hutchins, Y. Lao, K. Marsh, A. Moeller, Discovery of novel and highly selective inhibitors of calpain for the treatment of Alzheimer's disease: 2-(3-phenyl-1H-pyrazol-1-yl)-nicotinamides, J. Med. Chem. 60 (2017) 7123–7138, https://doi.org/10.1021/acs.jmedchem.7b00731.

[38] A. Dorababu, Indole-a promising pharmacophore in recent antiviral drug discovery, RSC Med. Chem. 11 (2020) 1335–1353, https://doi.org/10.1039/d0md00288g.

[39] N.A. Meanwell, M.R. Krystal, B. Nowicka-Sans, D.R. Langley, D.A. Conlon, M. D. Eastgate, D.M. Grasela, P. Timmins, T. Wang, J.F. Kadow, Inhibitors of HIV-1 attachment: the discovery and development of temsavir and its prodrug fostemsavir, J. Med. Chem. 61 (2018) 62–80, https://doi.org/10.1021/acs.jmedchem.7b01337.

[40] N. Ruwizhi, B.A. Aderibigbe, Cinnamic acid derivatives and their biological efficacy, Int. J. Mol. Sci. 21 (2020) 1–36, https://doi.org/10.3390/ijms21165712.

[41] O.M. Abd El-Raouf, E.S.M. El-Sayed, M.F. Manie, Cinnamic acid and cinnamaldehyde ameliorate cisplatin-induced splenotoxicity in rats, J. Biochem. Mol. Toxicol. 29 (2015) 426–431, https://doi.org/10.1002/jbt.21715.

[42] R. Wang, W. Yang, Y. Fan, W. Dehaen, Y. Li, H. Li, W. Wang, Q. Zheng, Q. Huai, Design and synthesis of the novel oleanolic acid-cinnamic acid ester derivatives and glycyrrhetinic acid-cinnamic acid ester derivatives with cytotoxic properties, Bioorg. Chem. 88 (2019), 102951, https://doi.org/10.1016/j.bioorg.2019.102951.

[43] S. Guo, Y. Zhen, Z. Zhu, G. Zhou, X. Zheng, Cinnamic acid rescues behavioral deficits in a mouse model of traumatic brain injury by targeting miR-455-3p/HDAC2, Life Sci. 235 (2019), 116819, https://doi.org/10.1016/j.lfs.2019.116819.

[44] R. Amano, A. Yamashita, H. Kasai, T. Hori, S. Miyasato, S. Saito, H. Yokoe, K. Takahashi, T. Tanaka, T. Otoguro, S. Maekawa, N. Enomoto, M. Tsubuki, K. Moriishi, Cinnamic acid derivatives inhibit hepatitis C virus replication via the induction of oxidative stress, Antiviral Res. 145 (2017) 123–130, https://doi.org/10.1016/j.antiviral.2017.07.018.

[45] A.M. Faucher, M.D. Bailey, P.L. Beaulieu, C. Brochu, J.S. Duceppe, J.M. Ferland, E. Ghiro, V. Gorys, T. Halmos, S.H. Kawai, M. Poirier, B. Simoneau, Y.S. Tsantrizos, M. Llinàs-Brunet, Synthesis of BILN 2061, an HCV NS3 protease inhibitor with proven antiviral effect in humans, Org. Lett. 6 (2004) 2901–2904, https://doi.org/10.1021/ol0489907.

[46] Y. Chen, Z. Li, P. Pan, Z. Lao, J. Xu, Z. Li, S. Zhan, X. Liu, Y. Wu, W. Wang, G. Li, Cinnamic acid inhibits Zika virus by inhibiting RdRp activity, Antiviral Res. 192 (2021), 105117, https://doi.org/10.1016/j.antiviral.2021.105117.

[47] F. Li, E.M. Lee, X. Sun, D. Wang, H. Tang, G.C. Zhou, Design, synthesis and discovery of andrographolide derivatives against Zika virus infection, Eur. J. Med. Chem. 187 (2020), 111925, https://doi.org/10.1016/j.ejmech.2019.111925.

[48] G. Barbosa-Lima, A.M. Moraes, A. da S. Araújo, E.T. da Silva, C.S. de Freitas, Y. R. Vieira, A. Marttorelli, J.C. Neto, P.T. Bozza, M.V.N. de Souza, T.M.L. Souza, 2,8-bis(trifluoromethyl)quinoline analogs show improved anti-Zika virus activity,

compared to mefloquine, Eur. J. Med. Chem. 127 (2017) 334–340, https://doi.org/10.1016/j.ejmech.2016.12.058.
[49] A. Balasubramanian, T. Teramoto, A.A. Kulkarni, A.K. Bhattacharjee, R. Padmanabhan, Antiviral activities of selected antimalarials against dengue virus type 2 and Zika virus, Antiviral Res. 137 (2017) 141–150, https://doi.org/10.1016/j.antiviral.2016.11.015.
[50] C. Nitsche, M.A.M. Behnam, C. Steuer, C.D. Klein, Retro peptide-hybrids as selective inhibitors of the Dengue virus NS2B-NS3 protease, Antiviral Res. 94 (2012) 72–79, https://doi.org/10.1016/j.antiviral.2012.02.008.
[51] C. Nitsche, C. Steuer, C.D. Klein, Arylcyanoacrylamides as inhibitors of the Dengue and West Nile virus proteases, Bioorg. Med. Chem. 19 (2011) 7318–7337, https://doi.org/10.1016/j.bmc.2011.10.061.
[52] C. de la Guardia, D.E. Stephens, H.T. Dang, M. Quijada, O.V. Larionov, R. Lleonart, Antiviral activity of novel quinoline derivatives against dengue virus serotype 2, Molecules. 23 (2018) 1–11, https://doi.org/10.3390/molecules23030672.
[53] S.J.F. Kaptein, P. Vincetti, E. Crespan, J.I.A. Rivera, G. Costantino, G. Maga, J. Neyts, M. Radi, Identification of broad-spectrum dengue/zika virus replication inhibitors by functionalization of quinoline and 2,6-diaminopurine scaffolds, ChemMedChem. 13 (2018) 1371–1376, https://doi.org/10.1002/cmdc.201800178.
[54] J. Deng, N. Li, H. Liu, Z. Zuo, O.W. Liew, W. Xu, G. Chen, X. Tong, W. Tang, J. Zhu, J. Zuo, H. Jiang, C.G. Yang, J. Li, W. Zhu, Discovery of novel small molecule inhibitors of dengue viral NS2B-NS3 protease using virtual screening and scaffold hopping, J. Med. Chem. 55 (2012) 6278–6293, https://doi.org/10.1021/jm300146f.
[55] H. Beesetti, P. Tyagi, B. Medapi, V.S. Krishna, D. Sriram, N. Khanna, S. Swaminathan, A quinoline compound inhibits the replication of dengue virus serotypes 1–4 in Vero cells, Antivir. Ther. 23 (2018) 385–394, https://doi.org/10.3851/IMP3231.
[56] J. Zhao, Y. Zhang, M. Wang, Q. Liu, X. Lei, M. Wu, S. Guo, D. Yi, Q. Li, L. Ma, Z. Liu, F. Guo, J. Wang, X. Li, Y. Wang, S. Cen, Quinoline and quinazoline derivatives inhibit viral RNA synthesis by SARS-CoV-2 RdRp, ACS Infect. Dis. 7 (2021) 1535–1544, https://doi.org/10.1021/acsinfecdis.1c00083.
[57] E.D. Micewicz, R. Khachatoorian, S.W. French, P. Ruchala, Identification of novel small-molecule inhibitors of Zika virus infection, Bioorg. Med. Chem. Lett. 28 (2018) 452–458, https://doi.org/10.1016/j.bmcl.2017.12.019.
[58] R. Khachatoorian, E.D. Micewicz, A. Micewicz, S.W. French, P. Ruchala, Optimization of 1,3-disubstituted urea-based inhibitors of Zika virus infection, Bioorg. Med. Chem. Lett. 29 (2019), 126626, https://doi.org/10.1016/j.bmcl.2019.126626.
[59] S. Mazzotta, T. Cebrero-Cangueiro, L. Frattaruolo, M. Vega-Holm, M. Carretero-Ledesma, J. Sánchez-Céspedes, A.R. Cappello, F. Aiello, J. Pachón, J.M. Vega-Pérez, F. Iglesias-Guerra, M.E. Pachón-Ibáñez, Exploration of piperazine-derived thioureas as antibacterial and anti-inflammatory agents. In vitro evaluation against clinical isolates of colistin-resistant Acinetobacter baumannii, Bioorganic Med, Chem. Lett. 30 (2020), 127411, https://doi.org/10.1016/j.bmcl.2020.127411.
[60] J.G. Moffat, J. Rudolph, D. Bailey, Phenotypic screening in cancer drug discovery-past, present and future, Nat. Rev. Drug Discov. 13 (2014) 588–602, https://doi.org/10.1038/nrd4366.
[61] S.A. Shiryaev, C. Farhy, A. Pinto, C.T. Huang, N. Simonetti, A.E. Ngono, A. Dewing, S. Shresta, A.B. Pinkerton, P. Cieplak, A.Y. Strongin, A.V. Terskikh, Characterization of the Zika virus two-component NS2B-NS3 protease and structure-assisted identification of allosteric small-molecule antagonists, Antiviral Res. 143 (2017) 218–229, https://doi.org/10.1016/j.antiviral.2017.04.015.
[62] L. Papageorgiou, S. Loukatou, K. Sofia, D. Maroulis, D. Vlachakis, An updated evolutionary study of Flaviviridae NS3 helicase and NS5 RNA-dependent RNA polymerase reveals novel invariable motifs as potential pharmacological targets, Mol. Biosyst. 12 (2016) 2080–2093, https://doi.org/10.1039/c5mb00706b.
[63] D. Luo, S.G. Vasudevan, J. Lescar, The flavivirus NS2B-NS3 protease-helicase as a target for antiviral drug development, Antiviral Res. 118 (2015) 148–158, https://doi.org/10.1016/j.antiviral.2015.03.014.
[64] C. Caillet-Saguy, S.P. Lim, P.Y. Shi, J. Lescar, S. Bressanelli, Polymerases of hepatitis C viruses and flaviviruses: structural and mechanistic insights and drug development, Antiviral Res. 105 (2014) 8–16, https://doi.org/10.1016/j.antiviral.2014.02.006.
[65] Y. Yang, L. Cao, H. Gao, Y. Wu, Y. Wang, F. Fang, T. Lan, Z. Lou, Y. Rao, Discovery, optimization, and target identification of novel potent broad-spectrum antiviral inhibitors, J. Med. Chem. 62 (2019) 4056–4073, https://doi.org/10.1021/acs.jmedchem.9b00091.
[66] I. Vicenti, F. Dragoni, A. Giannini, F. Giammarino, M. Spinicci, F. Saladini, A. Boccuto, M. Zazzi, Development of a cell-based immunodetection assay for simultaneous screening of antiviral compounds inhibiting zika and dengue virus replication, SLAS Discov. 25 (2020) 506–514, https://doi.org/10.1177/2472555220911456.
[67] A. Brai, A. Boccuto, M. Monti, S. Marchi, I. Vicenti, F. Saladini, C.I. Trivisani, A. Pollutri, C.M. Trombetta, E. Montomoli, V. Riva, A. Garbelli, E.M. Nola, M. Zazzi, G. Maga, E. Dreassi, M. Botta, Exploring the Implication of DDX3X in DENV infection: discovery of the first-in-class DDX3X fluorescent inhibitor, ACS Med. Chem. Lett. 11 (2020) 956–962, https://doi.org/10.1021/acsmedchemlett.9b00681.
[68] I. Vicenti, A. Boccuto, A. Giannini, F. Dragoni, F. Saladini, M. Zazzi, Comparative analysis of different cell systems for Zika virus (ZIKV) propagation and evaluation of anti-ZIKV compounds in vitro, Virus Res. 244 (2018) 64–70, https://doi.org/10.1016/j.virusres.2017.11.003.
[69] C.Q. Sacramento, G.R. De Melo, C.S. De Freitas, N. Rocha, L.V.B. Hoelz, M. Miranda, N. Fintelman-Rodrigues, A. Marttorelli, A.C. Ferreira, G. Barbosa-Lima, J.L. Abrantes, Y.R. Vieira, M.M. Bastos, E. De Mello Volotão, E.P. Nunes, D. A. Tschoeke, L. Leomil, E.C. Loiola, P. Trindade, S.K. Rehen, F.A. Bozza, P.T. Bozza, N. Boechat, F.L. Thompson, A.M.B. De Filippis, K. Brüning, T.M.L. Souza, The clinically approved antiviral drug sofosbuvir inhibits Zika virus replication, Sci. Rep. 7 (2017) 1–12, https://doi.org/10.1038/srep40920.
[70] H.N. Nagesh, A. Suresh, S.D.S.S. Sairam, D. Sriram, P. Yogeeswari, K.V.G. Chandra Sekhar, Design, synthesis and antimycobacterial evaluation of 1-(4-(2-substitutedthiazol-4-yl)phenethyl)-4-(3-(4-substitutedpiperazin-1-yl)alkyl) piperazine hybrid analogues, Eur. J. Med. Chem. 84 (2014) 605–613, https://doi.org/10.1016/j.ejmech.2014.07.067.
[71] M.F. Adasme, K.L. Linnemann, S.N. Bolz, F. Kaiser, S. Salentin, V.J. Haupt, M. Schroeder, PLIP 2021: Expanding the scope of the protein-ligand interaction profiler to DNA and RNA, Nucl. Acids Res. 49 (2021) W530–W534, https://doi.org/10.1093/nar/gkab294.
[72] L.L.C. Schrödinger, The PyMOL Molecular Graphics System, Version 1.8, 2015, (n. d.).
[73] A.N. Matthew, J. Zephyr, D. Nageswara Rao, M. Henes, W. Kamran, K. Kosovrasti, A.K. Hedger, G.J. Lockbaum, J. Timm, A. Ali, N. Kurt Yilmaz, C.A. Schiffer, Avoiding drug resistance by substrate envelope-guided design: toward potent and Robust HCV NS3/4A protease inhibitors, Mol. Biol. Physiol. 11 (2020) e00172–e220.
[74] V.S. Patil, D.R. Harish, U. Vetrivel, S. Roy, S.H. Deshpande, H.V. Hegde, Hepatitis C virus NS3/4A inhibition and host immunomodulation by tannins from terminalia chebula: a structural perspective, Molecules. 27 (2022), https://doi.org/10.3390/molecules27031076.
[75] J. Lei, G. Hansen, C. Nitsche, C.D. Klein, L. Zhang, R. Hilgenfeld, Crystal structure of zika virus NS2b-NS3 protease in complex with a boronate inhibitor, Science (80-.). 353 (2016) 503–505, https://doi.org/10.1126/science.aag2419.
[76] C.Y. Jia, J.Y. Li, G.F. Hao, G.F. Yang, A drug-likeness toolbox facilitates ADMET study in drug discovery, Drug Discov. Today. 25 (2020) 248–258, https://doi.org/10.1016/j.drudis.2019.10.014.
[77] C.A. Lipinski, F. Lombardo, B.W. Dominy, P.J. Feeney, Experimental and computational approaches to estimate solubility and permeability in drug discovery and development settings, Adv. Drug Deliv. Rev. 64 (2012) 4–17, https://doi.org/10.1016/j.addr.2012.09.019.
[78] D.F. Veber, S.R. Johnson, H.-Y. Cheng, B.R. Smith, K.W. Ward, K.D. Kopple, Molecular properties that influence the oral bioavailability of drug candidates, J. Med. Chem. 45 (2002) 2615–2623, https://doi.org/10.1021/jm020017n.
[79] R. Wang, Y. Fu, L. Lai, A New Method for Calculating Partition Coefficients of Organic Compounds, Acta Phys. - Chim. Sin. 13 (1997) 615–621, https://doi.org/10.3866/pku.whxb19970101.
[80] A. Daina, O. Michielin, V. Zoete, SwissADME: A free web tool to evaluate pharmacokinetics, drug-likeness and medicinal chemistry friendliness of small molecules, Sci. Rep. 7 (2017) 1–13, https://doi.org/10.1038/srep42717.
[81] N.H. Amin, M.T. El-Saadi, A.A. Ibrahim, H.M. Abdel-Rahman, Design, synthesis and mechanistic study of new 1,2,4-triazole derivatives as antimicrobial agents, Bioorg. Chem. 111 (2021), 104841, https://doi.org/10.1016/j.bioorg.2021.104841.
[82] M.M. Morcoss, E.S.M.N. Abdelhafez, R.A. Ibrahem, H.M. Abdel-Rahman, M. Abdel-Aziz, D.A. Abou El-Ella, Design, synthesis, mechanistic studies and in silico ADME predictions of benzimidazole derivatives as novel antifungal agents, Bioorg. Chem. 101 (2020), 103956, https://doi.org/10.1016/j.bioorg.2020.103956.
[83] P.F. Lamie, J.N. Philoppes, 2-Thiopyrimidine/chalcone hybrids: design, synthesis, ADMET prediction, and anticancer evaluation as STAT3/STAT5a inhibitors, J. Enzyme Inhib. Med. Chem. 35 (2020) 864–879, https://doi.org/10.1080/14756366.2020.1740922.
[84] S.K. Lee, Y. Kang, G.S. Chang, I.H. Lee, S.H. Park, J. Park, Bioinformatics and Molecular Design Research Center. Yonsei University, Seoul, (2017). <https://preadmet. bmdrc.kr>.
[85] V. Pogaku, K. Gangarapu, S. Basavoju, K.K. Tatapudi, S.B. Katragadda, Design, synthesis, molecular modelling, ADME prediction and anti-hyperglycemic evaluation of new pyrazole-triazolopyrimidine hybrids as potent α-glucosidase inhibitors, Bioorg. Chem. 93 (2019), 103307, https://doi.org/10.1016/j.bioorg.2019.103307.
[86] J. Sánchez-Céspedes, M.E. Pachón-Ibáñez, J. Pachón, P. Martínez-Aguado, T. Cebrero-Cangueiro, J.M. ega-Peréz, F. Iglesias-Guerra, M. Vega-Holm, J.I. Candela-Lena, S. Mazzotta, Piperazine derivatives as antiviral agents with increased therapeutic activity; year of application. EP16382073.1 (23 February 2016), US 2019/0308956 A1(10 October 2019).
[87] B.M. Minrovic, D. Jung, R.J. Melander, C. Melander, New class of adjuvants enables lower dosing of colistin against acinetobacter baumannii, ACS Infect. Dis. 4 (2018) 1368–1376, https://doi.org/10.1021/acsinfecdis.8b00103.
[88] P. Gallinari, D. Brennan, C. Nardi, M. Brunetti, L. Tomei, C. Steinkühler, R. De Francesco, Multiple enzymatic activities associated with recombinant NS3 protein of hepatitis C virus, J. Virol. 72 (1998) 6758–6769, https://doi.org/10.1128/jvi.72.8.6758-6769.1998.
[89] G. Barbato, D.O. Cicero, F. Cordier, F. Narjes, B. Gerlach, S. Sambucini, S. Grzesiek, V.G. Matassa, R. De Francesco, R. Bazzo, Inhibitor binding induces active site stabilization of the HCV NS3 protein serine protease domain, EMBO J. 19 (2000) 1195–1206, https://doi.org/10.1093/emboj/19.6.1195.
[90] D.L. Sali, R. Ingram, M. Wendel, D. Gupta, C. McNemar, A. Tsarbopoulos, J. W. Chen, Z. Hong, R. Chase, C. Risano, R. Zhang, N. Yao, A.D. Kwong, L. Ramanathan, H.V. Le, P.C. Weber, Serine protease of hepatitis C virus expressed in insect cells as the NS3/4A complex, Biochemistry. 37 (1998) 3392–3401, https://doi.org/10.1021/bi972010r.

[91] X. Tong, R. Chase, A. Skelton, T. Chen, J. Wright-Minogue, B.A. Malcolm, Identification and analysis of fitness of resistance mutations against the HCV protease inhibitor SCH 503034, Antiviral Res. 70 (2006) 28–38, https://doi.org/10.1016/j.antiviral.2005.12.003.

[92] P. Gallego, Á. Rojas, G. Falcón, P. Carbonero, M.R. García-Lozano, A. Gil, L. Grande, O. Cremades, M. Romero-Gómez, J.D. Bautista, J.A. Del Campo, Water-soluble extracts from edible mushrooms (: Agaricus bisporus) as inhibitors of hepatitis C viral replication, Food Funct. 10 (2019) 3758–3767, https://doi.org/10.1039/c9fo00733d.

[93] U.W. Hawas, R. Al-Farawati, L.T.A. El-Kassem, A.J. Turki, Different culture metabolites of the Red Sea fungus Fusarium equiseti optimize the inhibition of hepatitis C virus NS3/4A protease (HCV PR), Mar. Drugs. 14 (2016), https://doi.org/10.3390/md14100190.

[94] H.M.L.J. Reed, A simple method of estimating fifty per cent endpoints, Am. J. Hyg. 27 (1938) 546–558, https://doi.org/10.7723/antiochreview.72.3.0546.

[95] N.M. O'Boyle, M. Banck, C.A. James, C. Morley, T. Vandermeersch, G. R. Hutchison, Open babel, J. Cheminform. 3 (2011) 1–14, https://doi.org/10.1186/1758-2946-3-33.

[96] O.V. Stroganov, F.N. Novikov, V.S. Stroylov, V. Kulkov, G.G. Chilov, Lead finder: an approach to improve accuracy of protein-ligand docking, binding energy estimation, and virtual screening, J. Chem. Inf. Model. 48 (2008) 2371–2385, https://doi.org/10.1021/ci800166p.